OSA Webinar: Plasma Photonic Crystals and the Tunable Parameters Control of the Bandgaps

Presenter: Matthew C. Paliwoda

Co-author: Joshua L. Rovey

Aerospace Engineering Department

University of Illinois Urbana-Champaign

Plasma Photonic Crystal

<u>Photonic Crystal:</u> A periodic structure near the wavelength of incident propagating wave that forms a dispersive material with bandgaps due to dielectric contrast between the structure's material.

<u>Atmospheric Plasma</u>:

A gas mixture of free electrons, ions, and neutrals with a net neutral charge and a pressure at or near 1 Earth atmosphere.

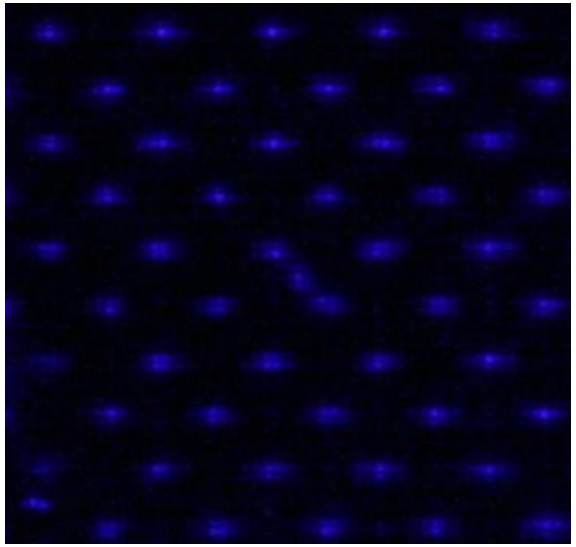

FIG 2. Top view: Imaged through ITO conductive glass. Down center of filaments

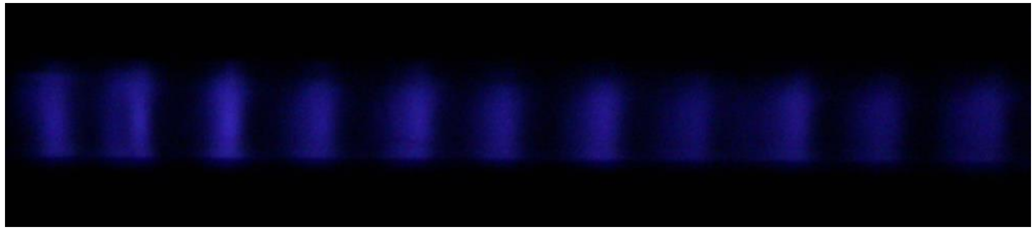

FIG 1. Side view: Plasma filaments formed in dielectric barrier discharge (DBD)

<u>Plasma Photonic Crystal:</u>
1D, 2D, and 3D structure formed from discharging plasma with a tunable dielectric constant and structure.

Plasma Photonic Crystal Advantages

<u>Capabilities</u>

Electrically tunable

- Structure
- Dielectric

$$\varepsilon_p(\omega_{pe}^2, \omega, \nu_c) = 1 - \frac{\omega_{pe}^2}{(\omega^2 - i\omega\nu_c)} \qquad \omega_{pe}^2 = \frac{n_e q^2}{m_e \varepsilon_o}$$

$$\varepsilon_p: [1, -\infty)$$

<u>Application</u>

- GHz – THz tunable components
- Durable periodic structures and metamaterials for High Power Microwaves[1]

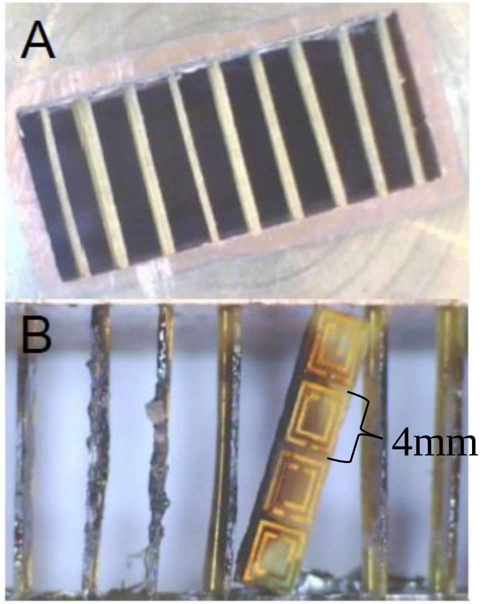

FIG 3. Effect of HPM on an array of split ring resonators: 1W 10GHz. Image of array (A) before (undamaged) and (B) after with scorch marks.[2]

Presentation Roadmap

1. Literature Review of Plasma Photonic Crystals (PPC)
2. Plane Wave Expansion Method (Simulation Model)
3. Controlling Parameter Trends
4. Reconfigurability Metrics Identify preferred parameters
5. Introduce PPC (Experiment) - Expanding bandgap control

1D PPC

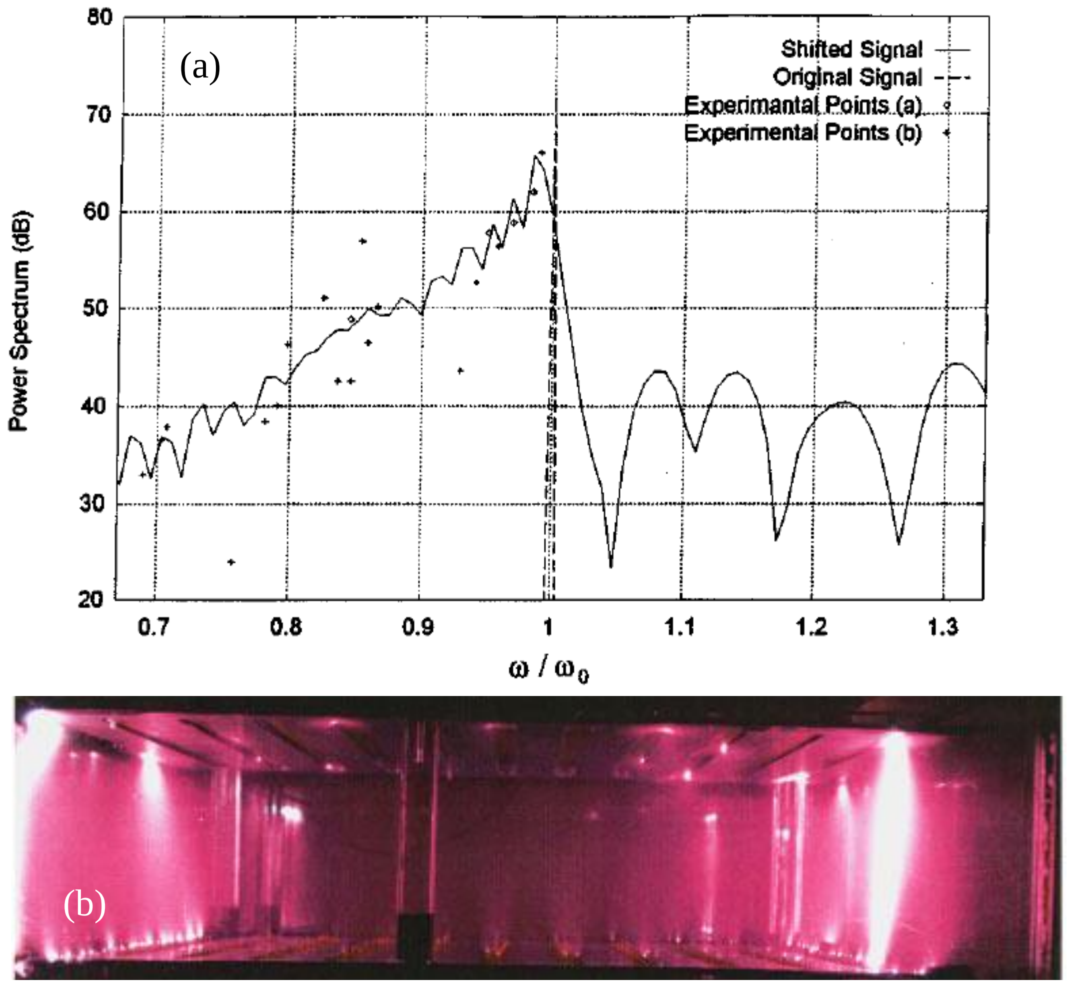

FIG 4. First Simulation and Demonstration of a PPC:
(a) Experimental and simulated power spectrum of (b) temporal 1D plasma sheets. **(**Faith, Kuo, and Huang) [3,4]

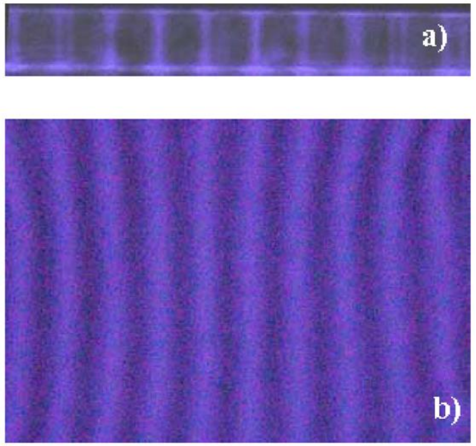

FIG. 5. 1D Filament DBD:
(Fan and Dong)[5]

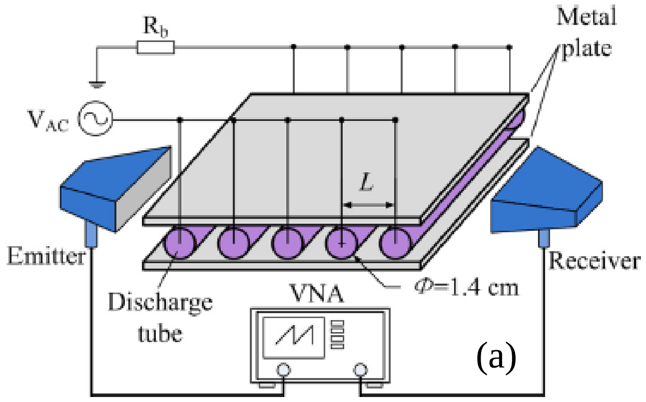

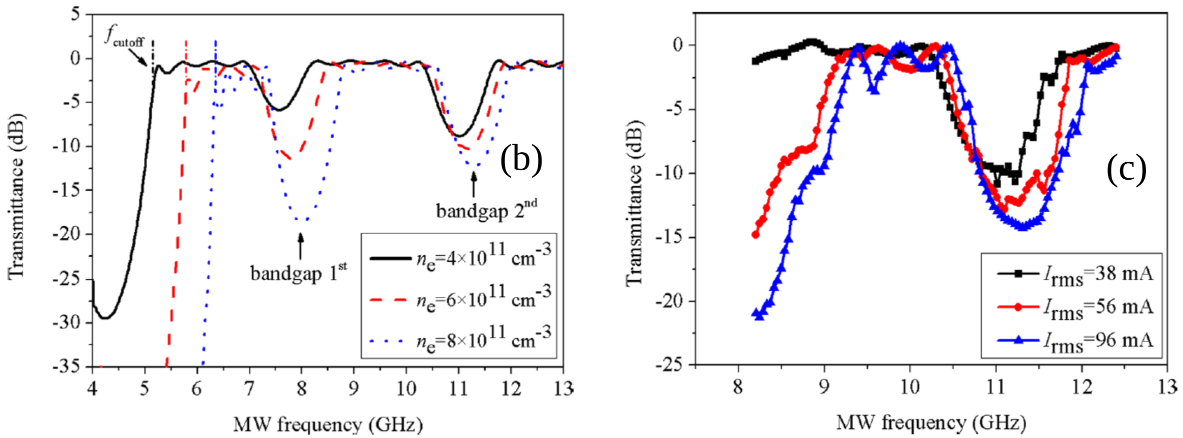

FIG. 6. Simulated and Experimental Bandgaps: (a) Setup Diagram, (b) Simulated, and (c) Experimental (Zhang and Ouyang)[6]

2D PPC

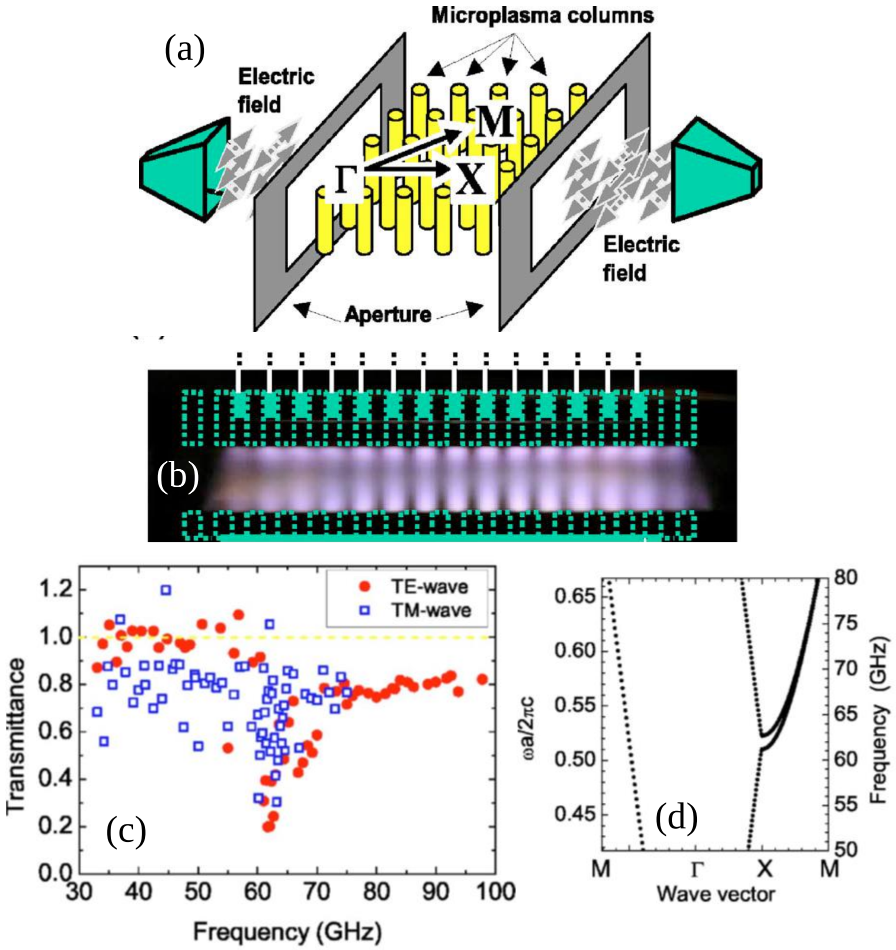

FIG. 7. First Demonstrated 2D PPC: Capillary jet DBD (a) Setup Diagram, (b) Discharge Image, (c) Experimental Results, and (d) Band Diagram (Sakai, Sakaguchi, and Tachibana)[7,8]

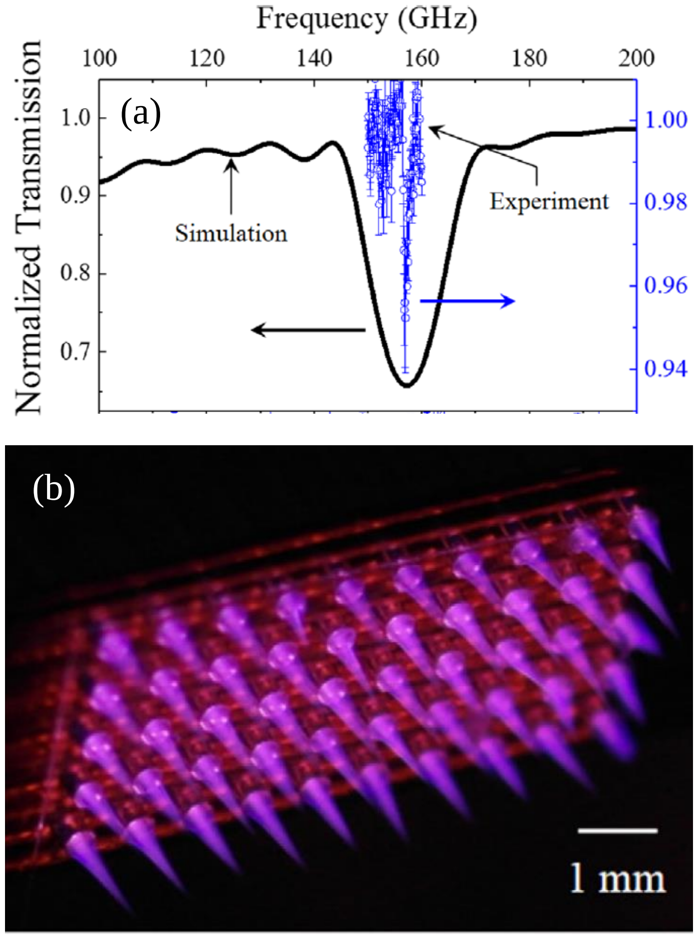

FIG. 8. Inductive Jet 2D PPC: (a) Simulation-experimental transmission data and (b) Discharge Image, (Yang, Park, and Eden)[9]

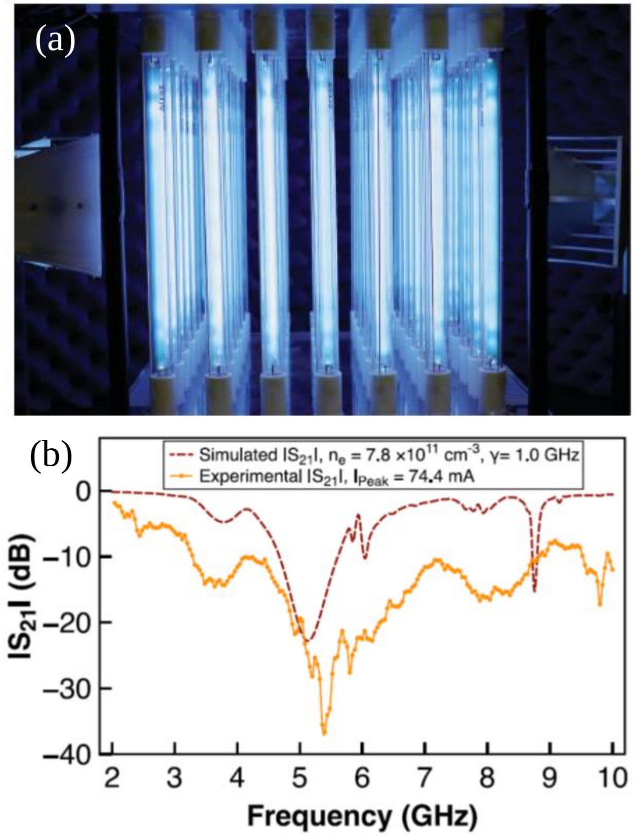

FIG. 9. Capillary 2D PPC: (a) Discharge simulation and (b) Simulation-experimental transmission data, (Wang and Cappelli)[10]

3D PPC

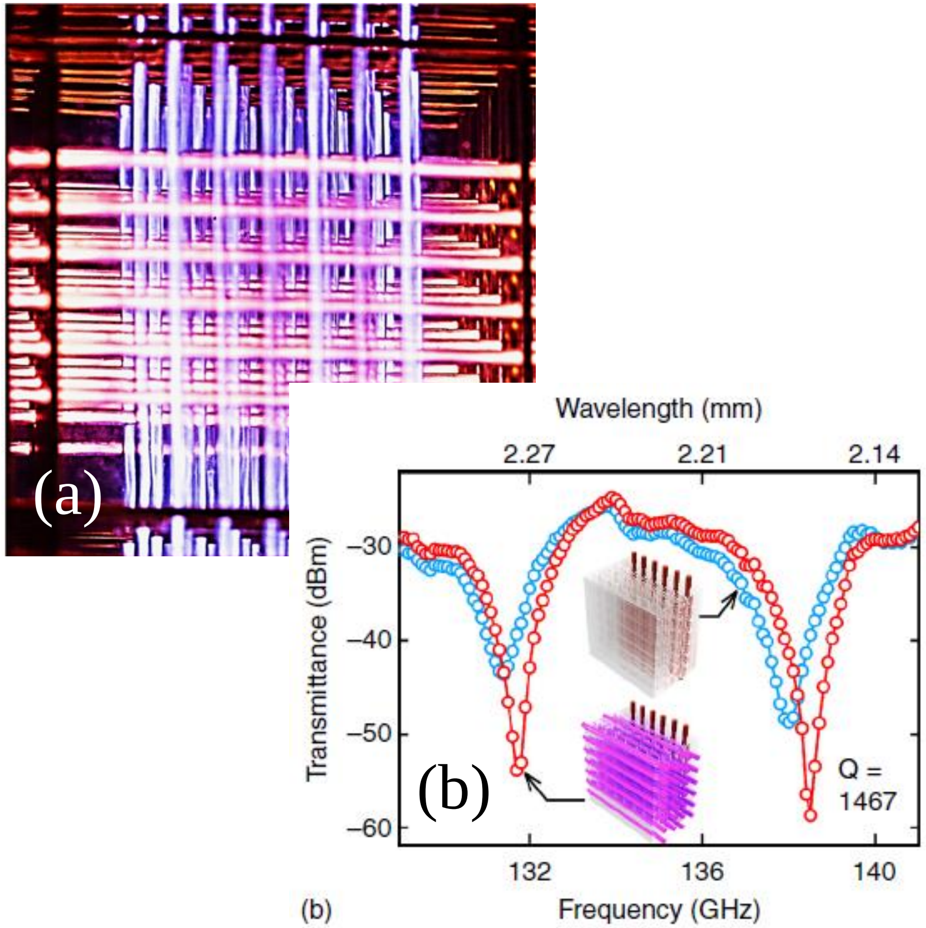

FIG 10. 3D Inductive Capillary PPC: (a) Discharge Image and (b) Experimental data with and without the plasma. (Sun, Zhang, Chen, Braun, and Eden)[11]

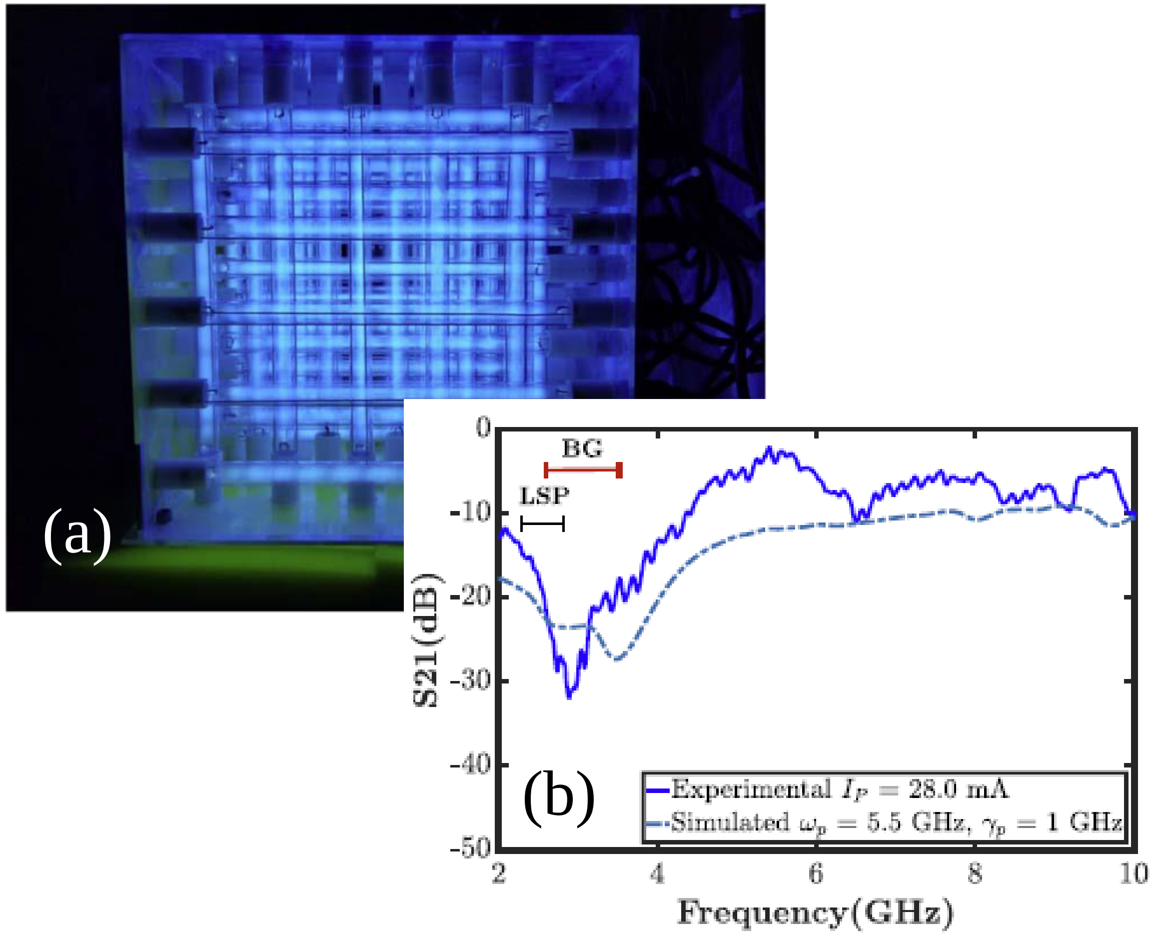

FIG 11. 3D Capacitive Discharge Capillary PPC: (a) Discharge Image and (b) experimental data and simulation. (Wang, Rodriguez, and Cappelli)[12]

Self-Organized PPC

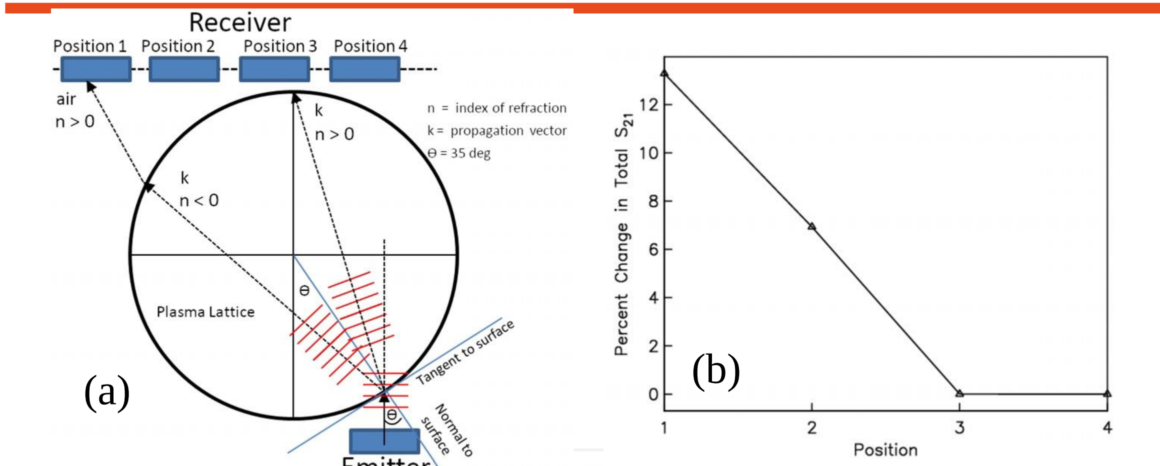
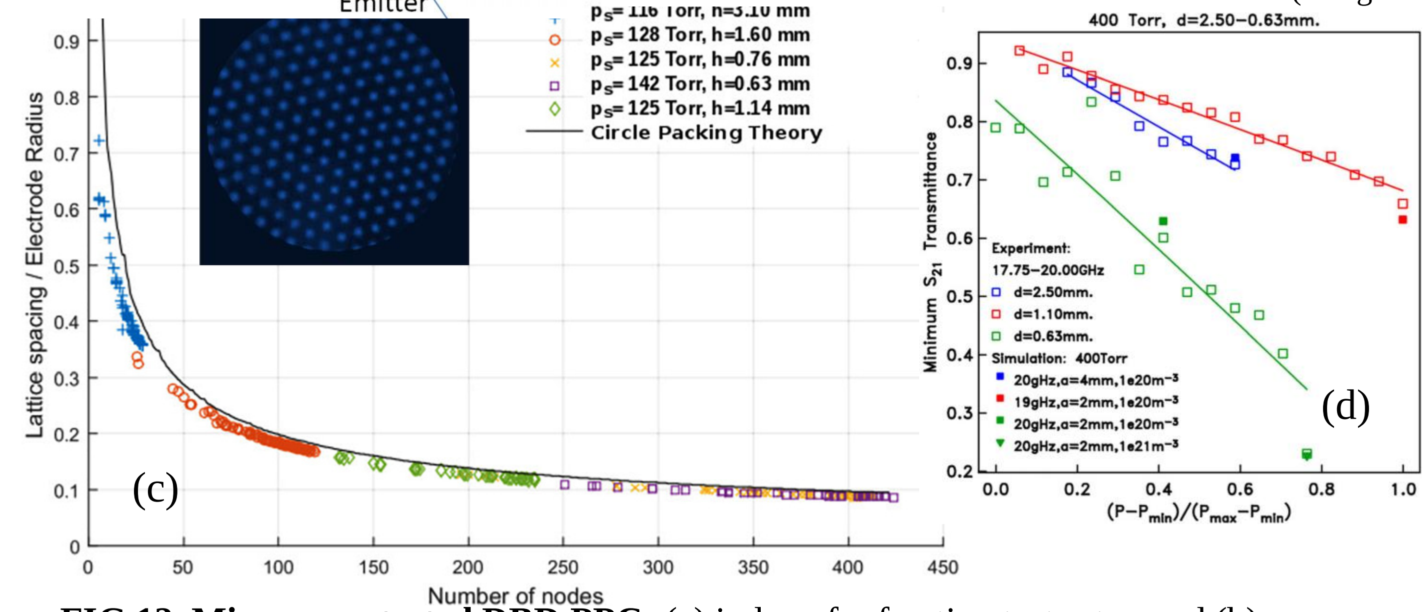

FIG 12. Microwave tested DBD PPC: (a) index of refraction test setup and (b) transmission change. (c) lattice constant parameter dependence. (d) transmission parameter dependence. (Matlis, Corke, Neiswander, and Hoffman)[13]

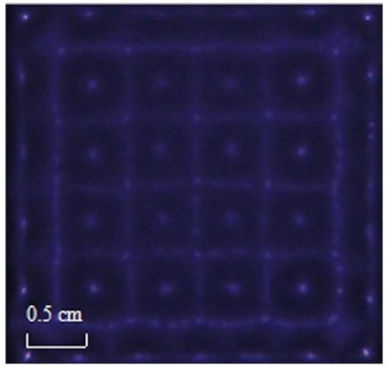

FIG 13. Square DBD Pattern (Dong et. al.)[14]

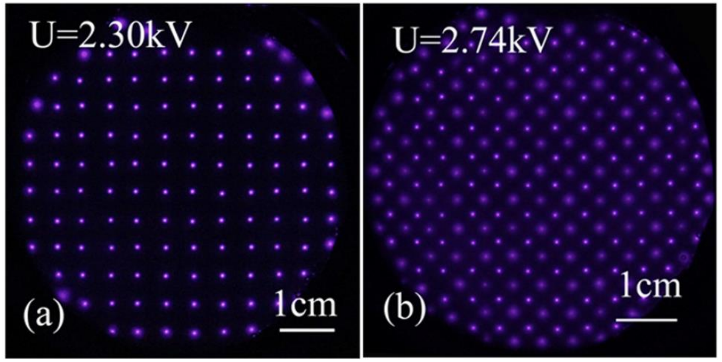

FIG 14, Forming (a) at electrodes and (b) between electrodes ((Dong et. al.) [15]

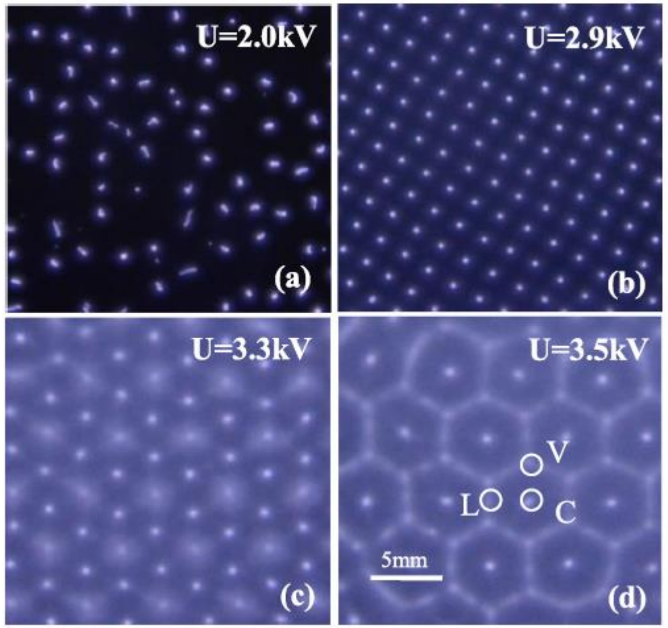

FIG 15. Evolution of DBD pattern with voltage: ((Dong et. al.) [16]

Waveguide PPC

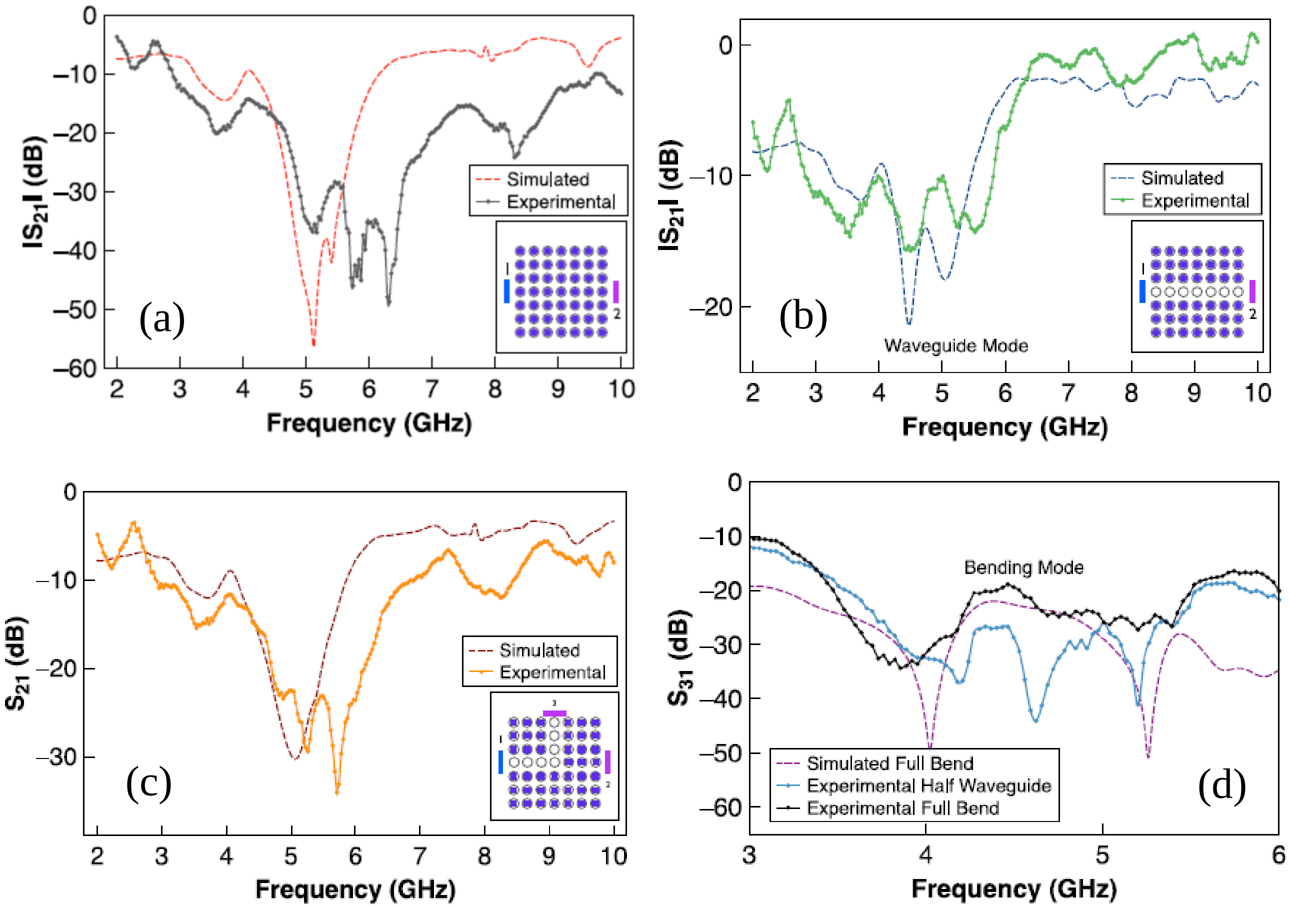

FIG 16. Experimental and simulated transmission through PPC waveguide: (a) all plasma on, (b) straight waveguide, (c) bent waveguide, and transmission to third port. (Wang and Cappelli)[10]

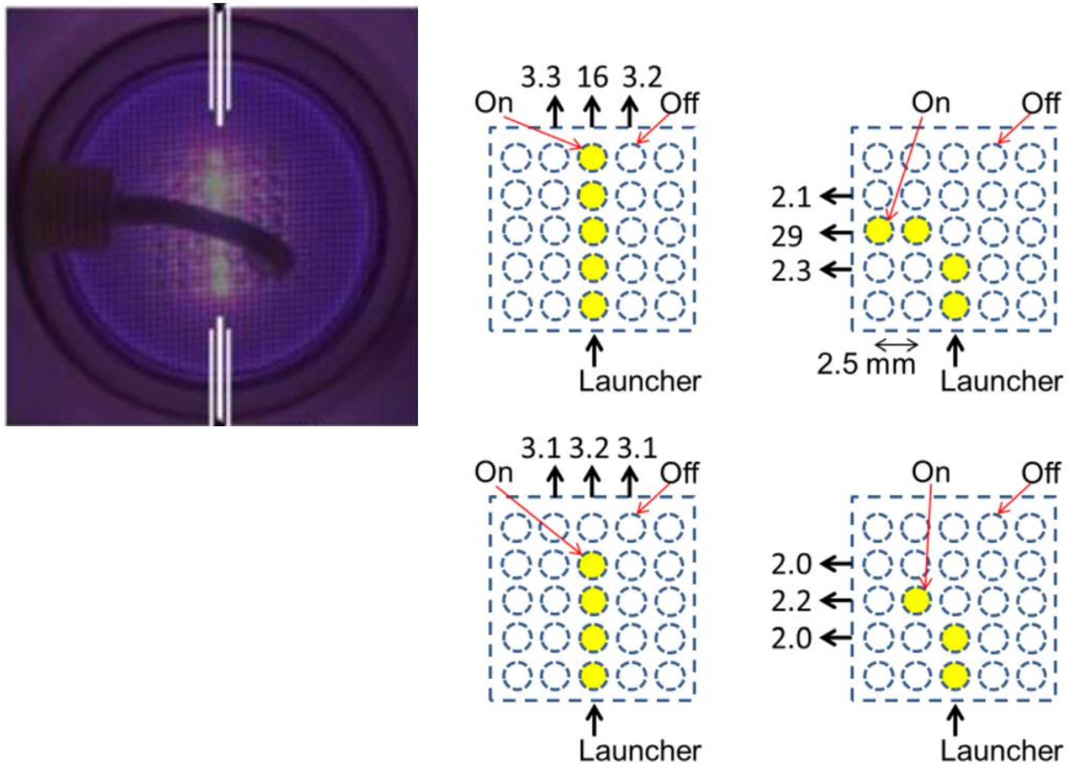

FIG 17. Plasmon waveguide on PPC: (a) Discharge image. Ratio of transmission with and without plasma (b) straight, (c) bent, (d) straight short, (e) bent short. (Sakai et. al) [17]

Simulated Complete Bandgaps and Negative Refraction

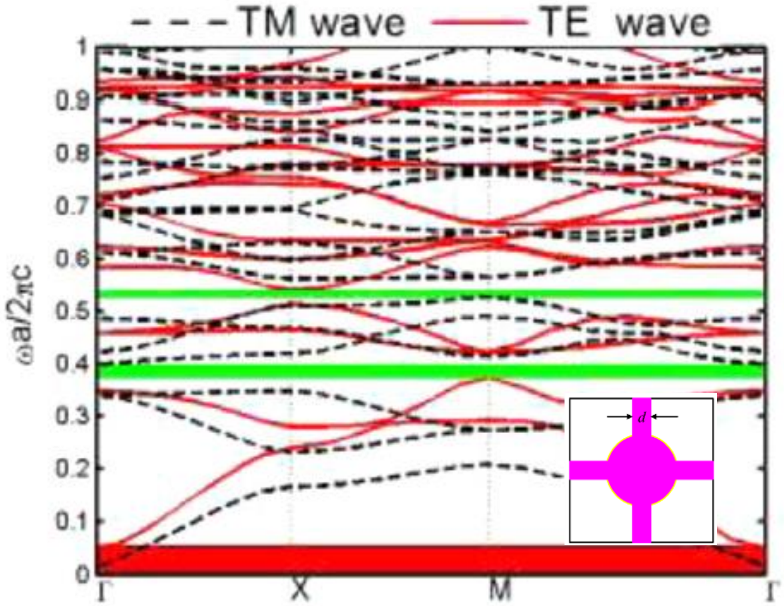

FIG 18. Complete bandgap: (H. F. Zhang et. al.)[18]

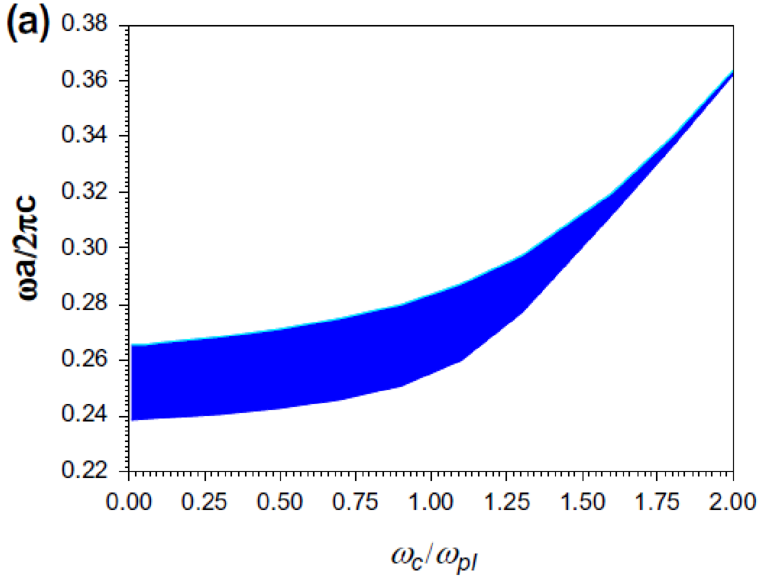

FIG 19. Normalized bandgap dependence on magnetic field: (H. F. Zhang et. al.)[19]

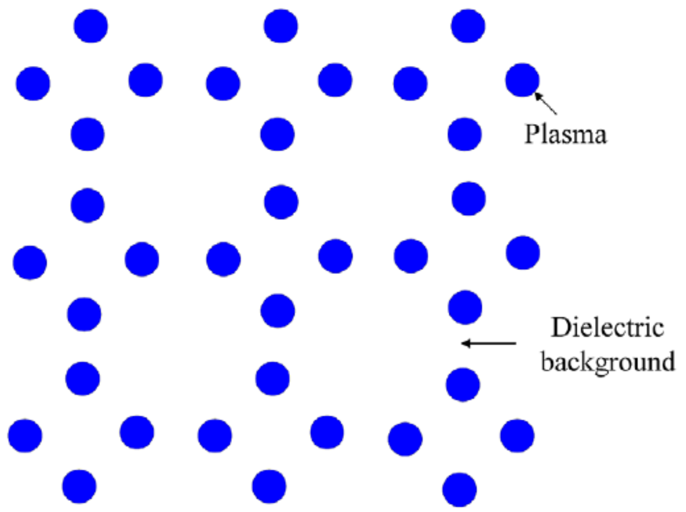

FIG 20. Pattern for all-angle negative refraction: (H. F. Zhang et. al.)[19]

Purpose of This Analysis[22]

- How do the bandgaps change with all possible parameters?
- How to quantitatively compare "Reconfigurability"?
- Which parameter is best for controlling a bandgap?
  - (Previous focus on plasma frequency and lattice constant)

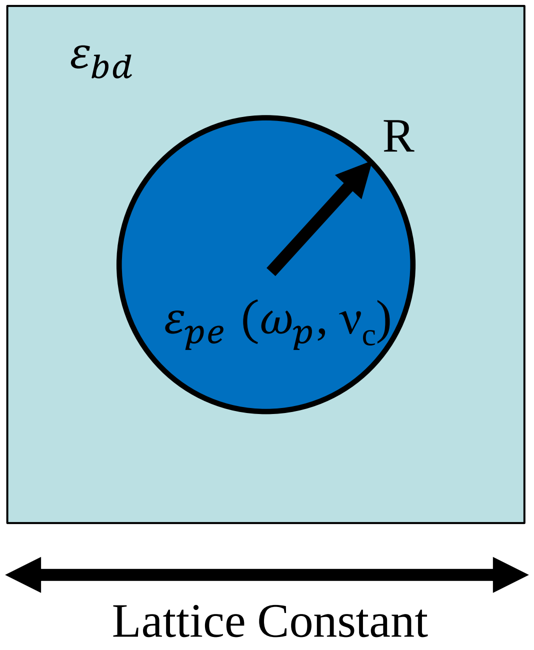

FIG 21. Unit Cell with Parameters

ε_{bd}:	Background Dielectric
ω_p:	Plasma Frequency
ν_c:	Collision Frequency
R:	Radius
a:	Lattice Constant

Plane Wave Expansion Method [23,24]

<u>Bloch Transform</u>

$$\boldsymbol{E}(\boldsymbol{x},\boldsymbol{k}) = \sum_{G} A(\boldsymbol{k},\boldsymbol{G})e^{i(\boldsymbol{k}+\boldsymbol{G})*\boldsymbol{x}}$$

$$\varepsilon(\boldsymbol{x},\omega) = \sum_{G'} \hat{\varepsilon}(\boldsymbol{G}',\omega)e^{i(\boldsymbol{G}')*\boldsymbol{x}}$$

$H_z = 0, \quad E_x = E_y = 0$

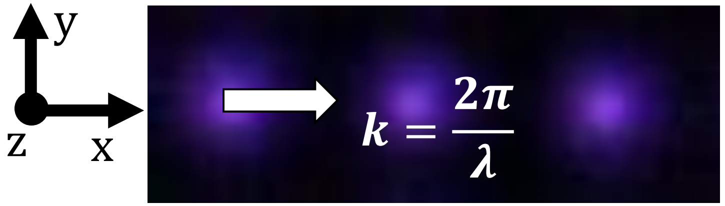

FIG 22. Propagation orientation in plasma columns

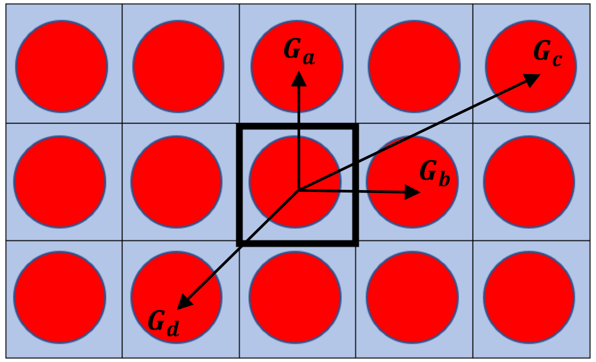

$$\boldsymbol{G_a} = \frac{2\pi}{a}\hat{\boldsymbol{y}}$$

$$\boldsymbol{G_b} = \frac{2\pi}{a}\hat{\boldsymbol{x}}$$

$$\boldsymbol{G_c} = \frac{4\pi}{a}\hat{\boldsymbol{x}} + \frac{2\pi}{a}\hat{\boldsymbol{y}}$$

$$\boldsymbol{G_d} = \frac{-2\pi}{a}\hat{\boldsymbol{x}} + \frac{-2\pi}{a}\hat{\boldsymbol{y}}$$

FIG 23. Examples of the Reciprocal Lattice Vector in Fourier Space

$$\boldsymbol{G} = \frac{2\pi n}{a}\,\hat{x} + \frac{2\pi m}{a}\,\hat{y}$$
$$m, n = 0, \pm 1, \pm 2, \pm 3 \ldots$$

<u>Helmholtz Equation – Fourier Space</u>

$$\nabla \times \left(\nabla \times \boldsymbol{E}(\boldsymbol{x},\boldsymbol{k})\right) - \left(\frac{\omega}{c}\right)^2 \varepsilon_{eff}(\boldsymbol{x})\boldsymbol{E}(\boldsymbol{x},\boldsymbol{k},\omega) = 0$$

<u>Combining equations and simplifying</u>

Summation Form: $\sum_{\boldsymbol{G}} (\boldsymbol{k}+\boldsymbol{G})^2 A(\boldsymbol{k},\boldsymbol{G})e^{i(\boldsymbol{k}+\boldsymbol{G})*\boldsymbol{x}} - \sum_{\boldsymbol{G}}\sum_{\boldsymbol{G}'} \hat{\varepsilon}(\boldsymbol{G}')A(\boldsymbol{k},\boldsymbol{G})e^{i(\boldsymbol{k}+\boldsymbol{G}'+\boldsymbol{G})*\boldsymbol{x}} = \boldsymbol{0}$

Simplified Matrix Form: $[\boldsymbol{1}]_{l\times l}[\,\boldsymbol{k}+\boldsymbol{G_l}]_{l\times l} - \left(\frac{\omega}{c}\right)^2 [\hat{\boldsymbol{\varepsilon}}(\boldsymbol{G}_l - \boldsymbol{G}_m)]_{l\times m} = [\boldsymbol{0}]$

Plane Wave Expansion Method

Each Term in Matrix

$$0 = -\delta_{lm}(\boldsymbol{k}+\boldsymbol{G_l})^2 + \left(\frac{\omega}{c}\right)^2 (\hat{\boldsymbol{\varepsilon}}_{\boldsymbol{lm}})$$

Kronecker Delta: δ_{lm}

$$0 = -\delta_{lm}(\boldsymbol{k}+\boldsymbol{G_l})^2 + \left(\frac{\omega}{c}\right)^2 \left(\theta_{lm} - \frac{\eta_{lm}}{(\omega^2 - i\omega\nu_c)}\right)$$

$$0 = \left(\frac{\omega}{c}\right)^3 \theta_{lm} - \left(\frac{\omega}{c}\right)^2 \frac{i\nu_c}{c}\theta_{lm} - \left(\frac{\omega}{c}\right)\left(\frac{\eta_{lm}}{c^2} + \delta_{lm}(\boldsymbol{k}+\boldsymbol{G_l})^2\right) + \frac{i\nu_c}{c}\delta_{lm}(\boldsymbol{k}+\boldsymbol{G_l})^2$$

Spatial Dielectric

$$\varepsilon(\boldsymbol{x},\omega) = \begin{cases} \varepsilon_{\mathrm{bg}}(\boldsymbol{x}) & , \ \textit{in the dielectric} \\ 1 - \dfrac{\omega_{pe}^2(\boldsymbol{x})}{(\omega^2 - i\omega\nu_c)}, & \textit{in the plasma} \end{cases}$$

Fourier Space Dielectric

$$\hat{\varepsilon}(\boldsymbol{G},\omega) = \frac{1}{S}\iint_S \varepsilon(\boldsymbol{x},\omega)\, \mathrm{e}^{-\mathrm{i}\mathbf{G}\cdot\mathbf{x}} dS$$

Linear Equation to Block Matrix

$$-\lambda^3\boldsymbol{X}_3 + \lambda^2\boldsymbol{X}_2 + \lambda\boldsymbol{X}_1 + \boldsymbol{X}_0 = \det\left[\underbrace{\begin{bmatrix} 0 & \boldsymbol{I} & 0 \\ 0 & 0 & \boldsymbol{I} \\ \boldsymbol{X}_0 & \boldsymbol{X}_1 & \boldsymbol{X}_2 \end{bmatrix}}_{Q} - \lambda \underbrace{\begin{bmatrix} \boldsymbol{I} & 0 & 0 \\ 0 & \boldsymbol{I} & 0 \\ 0 & 0 & \boldsymbol{X}_3 \end{bmatrix}}_{V}\right] = \boldsymbol{0}$$

Conditional Terms θ and η

$$\hat{\varepsilon}(\boldsymbol{G},\omega) = \theta(\boldsymbol{G}) - \frac{\eta(\boldsymbol{G})}{(\omega^2 - i\omega\nu_c)}$$

General Eigenvalue Problem

$$Qz - \lambda Vz = 0 \quad , \qquad \lambda = \left(\frac{\omega}{c}\right)$$

Final Function

$$func\big(\boldsymbol{k}, \omega_{pe}(\boldsymbol{x}), \varepsilon_{\mathrm{bg}}(\boldsymbol{x}), \boldsymbol{G}\big) = \omega$$

First non-linear dielectric PWE method by Kuzmiak and Maradudin[22] and later generalized by H. F. Zhang *et al*.[23]

Band Diagram

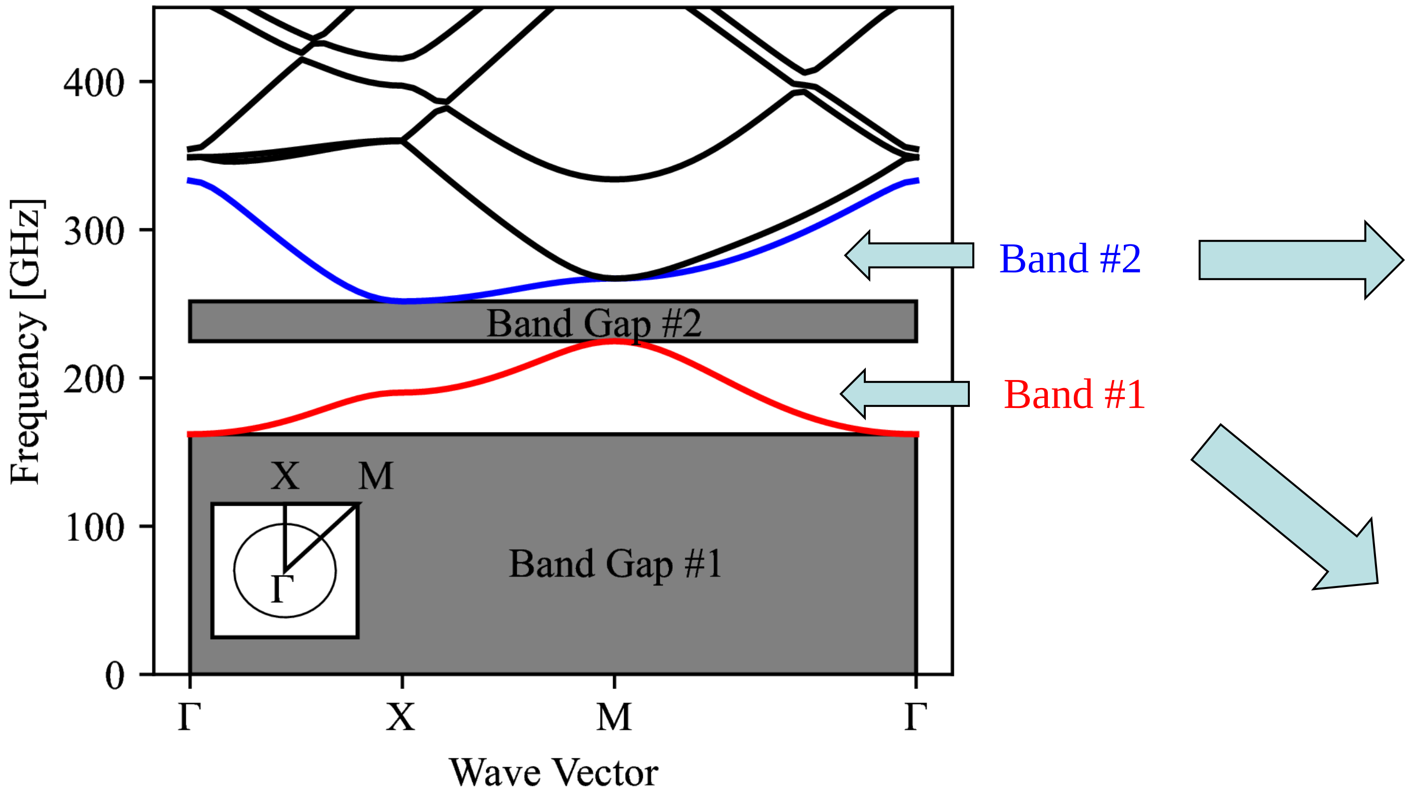

FIG 24. Band diagram (Example): The dispersion relationship (Frequency vs. Wavevector) for the series of wavevectors defined by the triangle perimeter, inscribe in the unit cell of the lower left corner. Each frequency line represents a harmonic solution to the Helmholtz Eq.

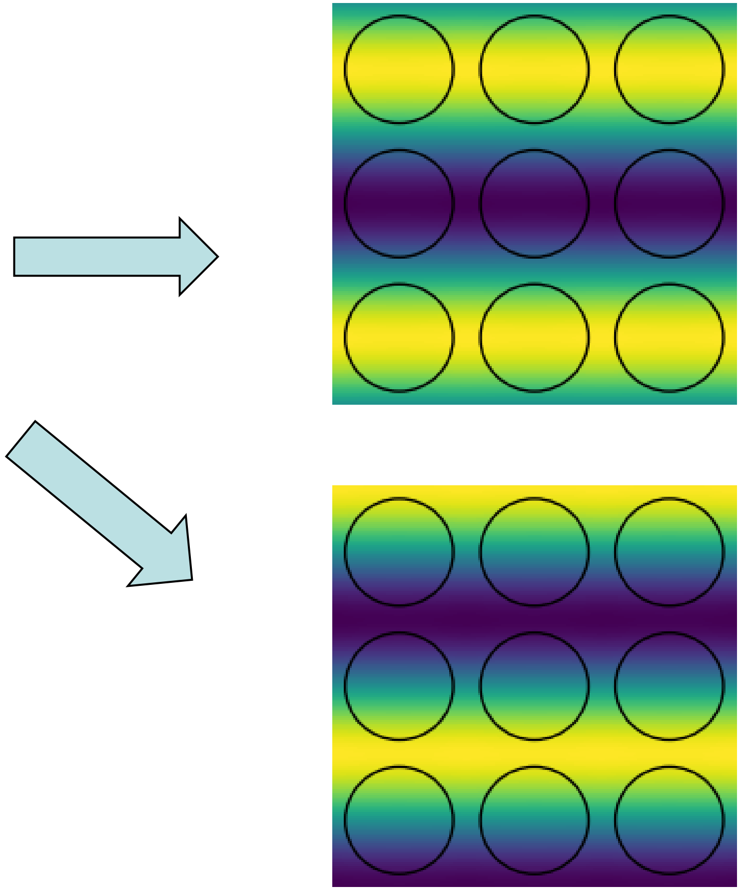

$$\frac{\omega}{k} = \frac{c}{\sqrt{\mu_r \varepsilon_r}}$$

FIG 25. Electric field distributions for the first two Bands (Example): Without bandgaps for clarity. Band #1 is concentrated in the background dielectric ($\varepsilon_{bd} \geq 1$) and Band #2 is concentrated in the plasma dielectric ($\varepsilon_{bd} \leq 1$).

Background Dielectric

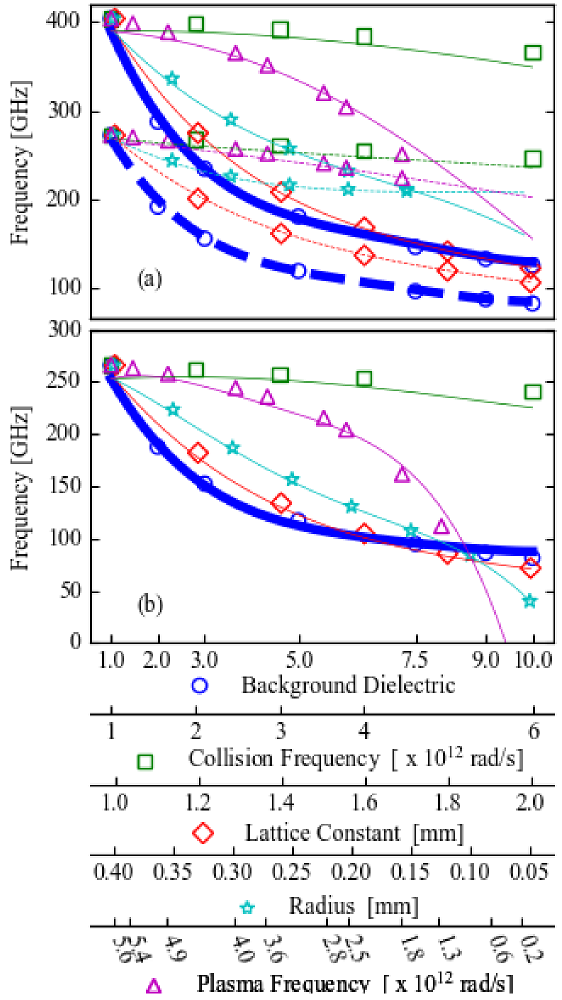

FIG 26. Parameter Trends: (a) Band Gap #2 and (b) Band Gap #1

$$\nabla \times (\nabla \times E(\boldsymbol{x}, \boldsymbol{k})) - \left(\frac{\omega}{c}\right)^2 \varepsilon(\boldsymbol{x}) E(\boldsymbol{x}, \boldsymbol{k}) = 0$$

$$\varepsilon(\boldsymbol{x}) = \varepsilon_{bg}$$

$$\omega = \sqrt{c^2 \frac{\nabla \times (\nabla \times E(\boldsymbol{x}, k))}{\varepsilon_{bg} E(\boldsymbol{x}, k)}}$$

$$\omega(\varepsilon_{bg}) \propto \frac{1}{\sqrt{\varepsilon_{bg}}}$$

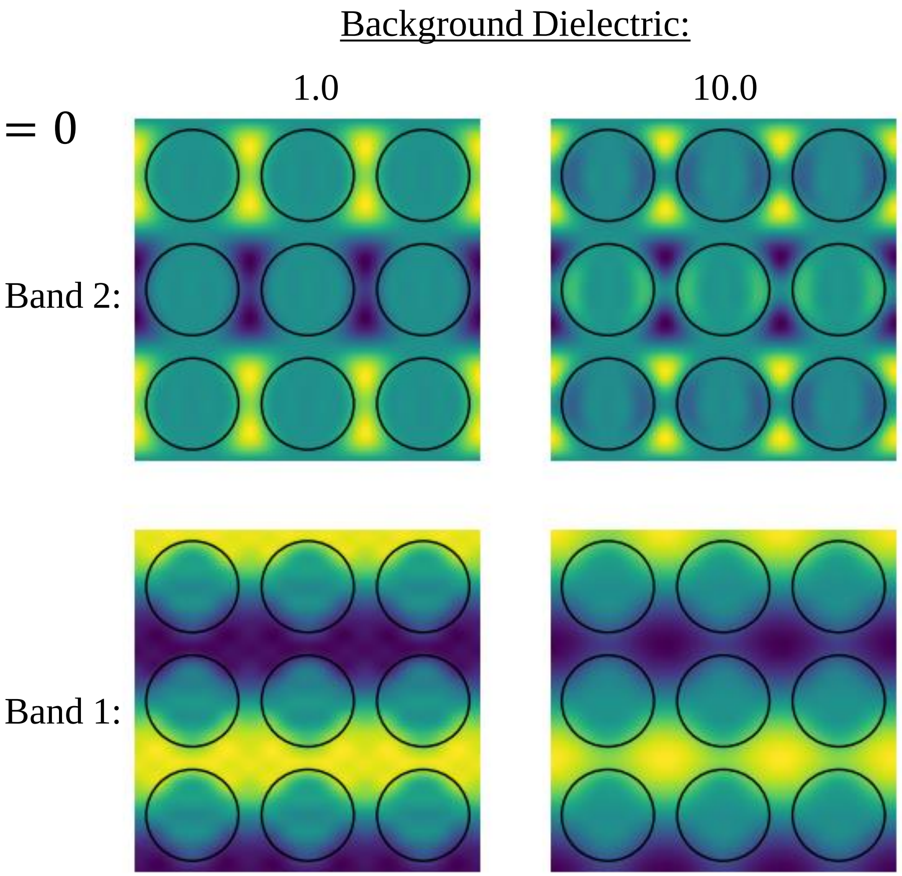

FIG 27. Electric field distributions of reference and final parameter value.

Wavevector along Γ-X, $k = \left\langle 0, \frac{\pi}{a} \right\rangle$

Plasma Frequency

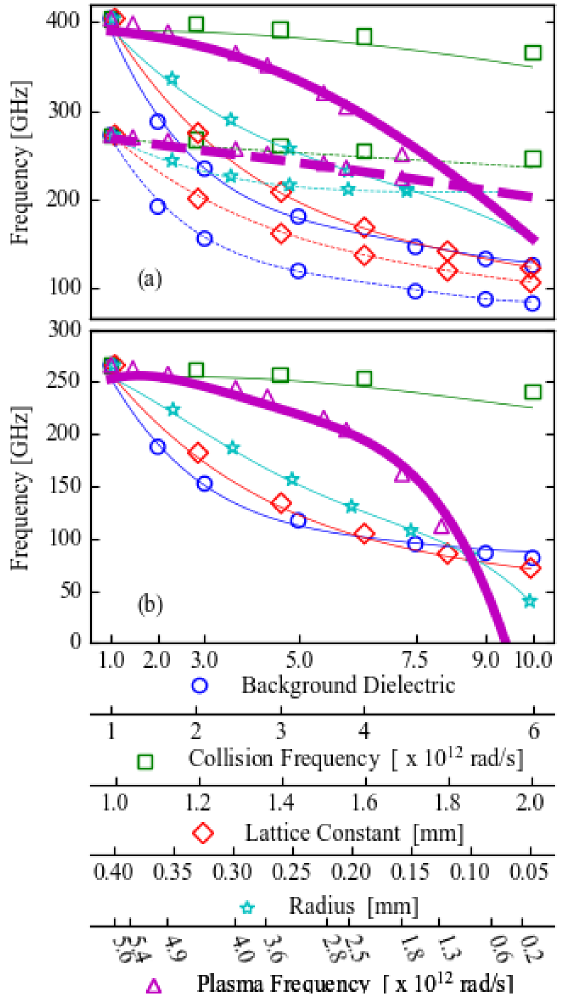

FIG 28. Parameter Trends: (a) Band Gap #2 and (b) Band Gap #1

$$\omega = \sqrt{c^2 \frac{\nabla \times (\nabla \times E(\boldsymbol{x}, k))}{\varepsilon(\boldsymbol{x}) E(\boldsymbol{x}, k)}}$$

$$\varepsilon = 1 - \frac{\omega_{pe}^2}{(\omega^2 - i\omega\nu_c)}$$

$$\omega = \pm \sqrt{\frac{1}{1 - \frac{\omega_{pe}^2}{(\omega^2 - i\omega\nu_c)}}} \sqrt{c^2 \frac{\nabla \times (\nabla \times E(\boldsymbol{x}, k))}{E(\boldsymbol{x}, k)}}$$

$$\omega(\omega_{pe}) \propto -\frac{1}{\omega_{pe}}$$

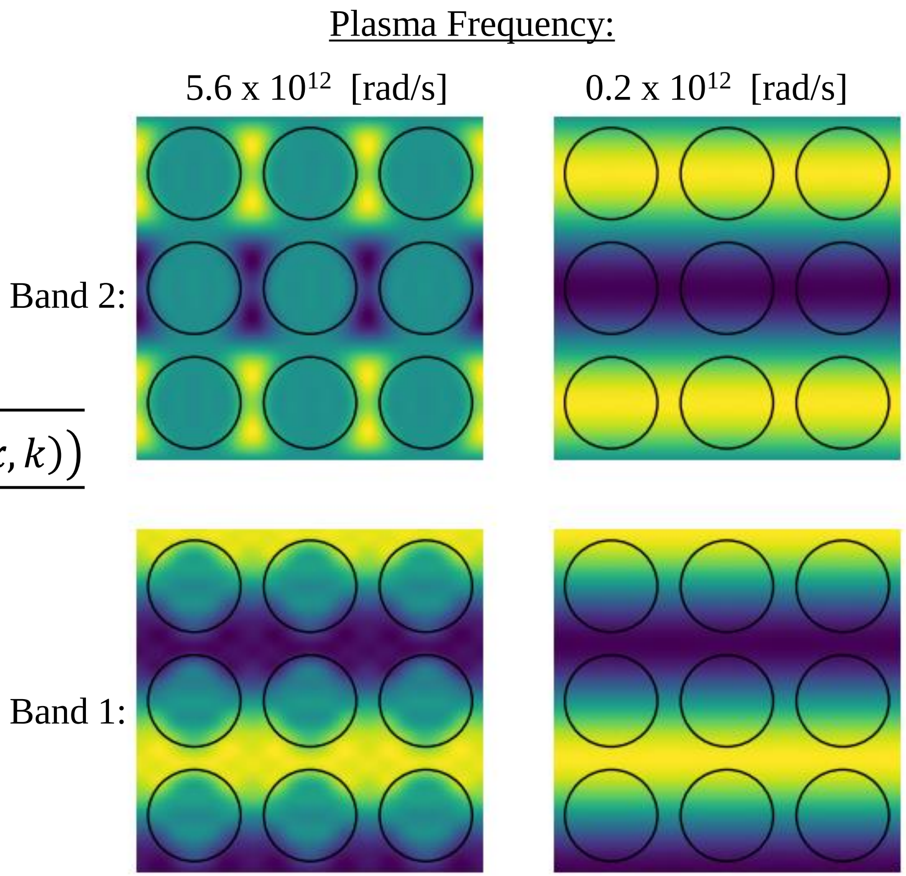

FIG 29. Electric field distributions of reference and final parameter value.

Wavevector along Γ-X, $k = \left\langle 0, \frac{\pi}{a} \right\rangle$

Collision Frequency

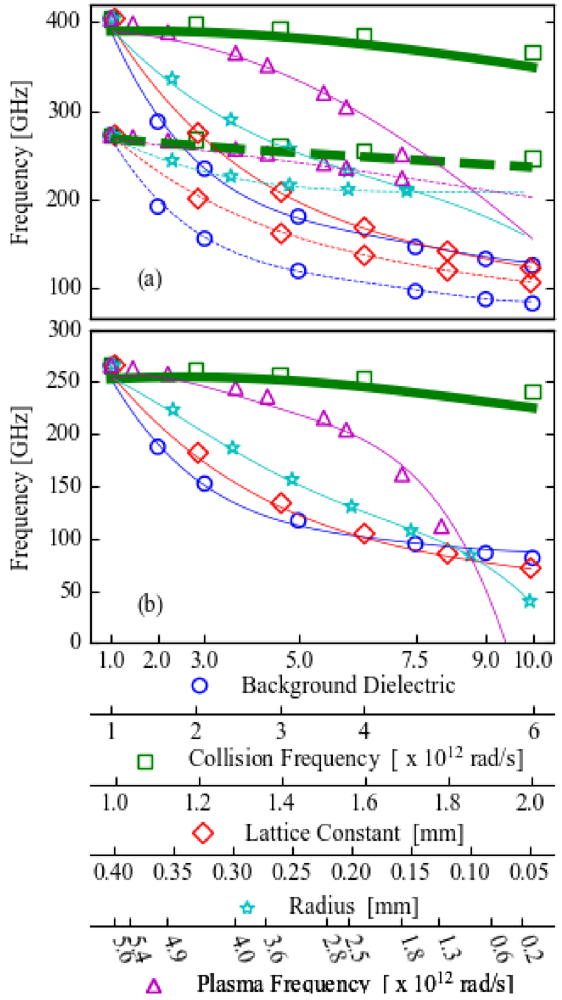

FIG 30. Parameter Trends: (a) Band Gap #2 and (b) Band Gap #1

$$\omega = \sqrt{\frac{1}{1-\frac{\omega_{pe}^2}{(\omega^2 - i\omega\nu_c)}}}\sqrt{c^2\frac{\nabla\times(\nabla\times E(\boldsymbol{x},k))}{E(\boldsymbol{x},k)}}$$

$$\omega = \pm\sqrt{\frac{\frac{\nu_c}{\omega}+1i}{\frac{\nu_c}{\omega}-i\frac{\omega_{pe}^2}{\omega^2}+1\mathrm{i}}}\sqrt{c^2\frac{\nabla\times(\nabla\times E(\boldsymbol{x},k))}{E(\boldsymbol{x},k)}}$$

$$\omega_{pe} \gg \omega$$

$$\frac{\nu_c}{\omega},\frac{\omega_{\mathrm{pe}}}{\omega} \gg 1i$$

$$\omega(\nu_c) \propto -\sqrt{\frac{1}{1-i\frac{\omega_{pe}^2}{\nu_c\omega}}}$$

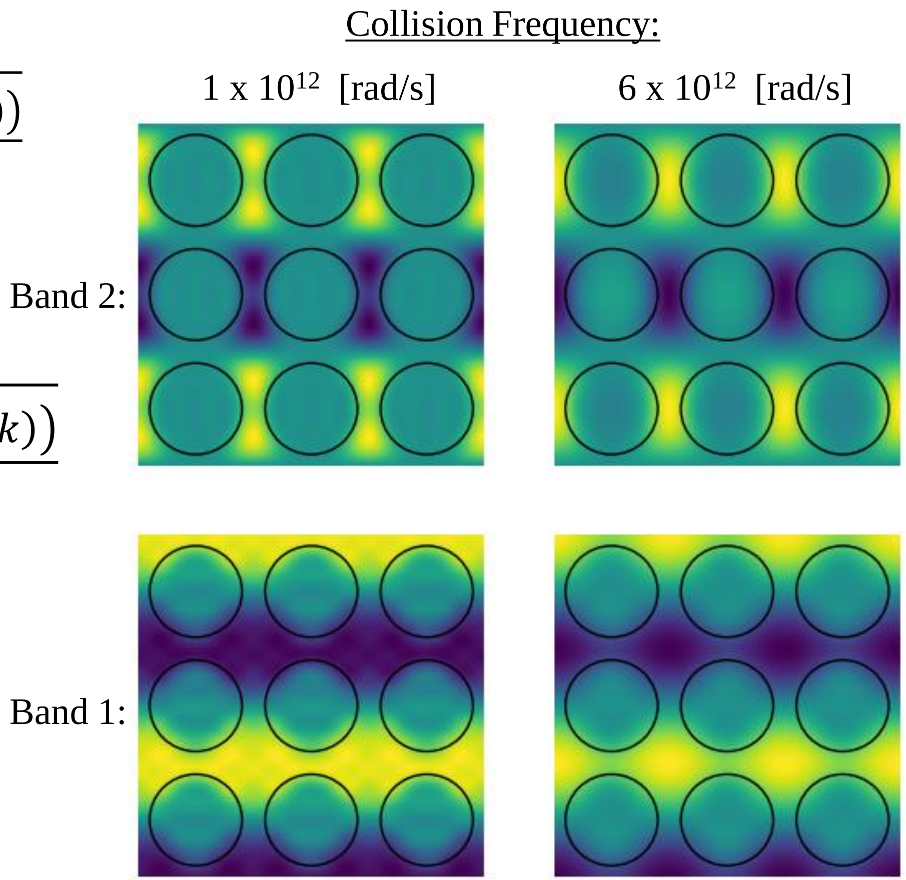

FIG 31. Electric field distributions of reference and final parameter value.

Wavevector along Γ-X, $k = \left\langle 0, \frac{\pi}{a} \right\rangle$

Column Radius

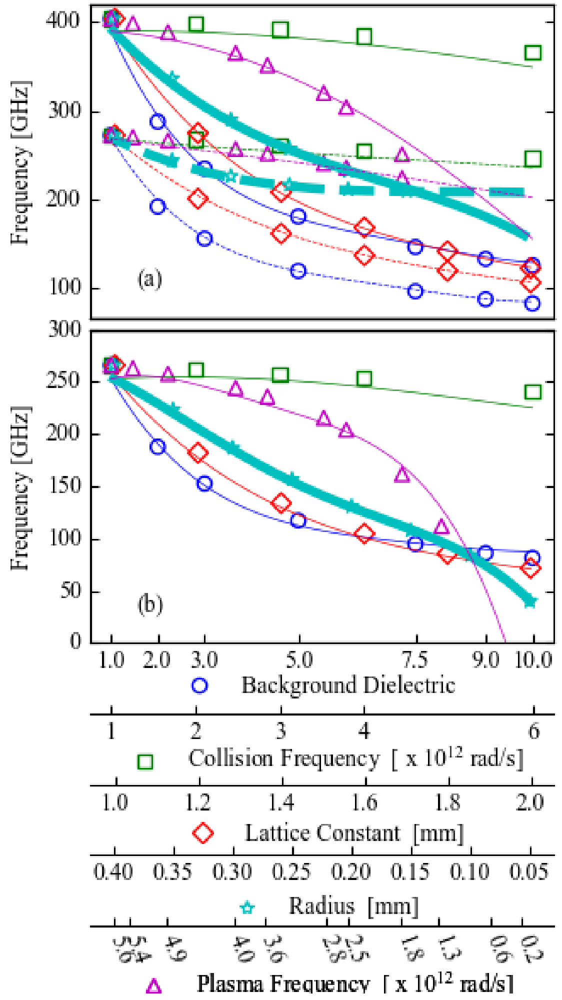

FIG 32. Parameter Trends: (a) Band Gap #2 and (b) Band Gap #1

$$\hat{\varepsilon}(\boldsymbol{G}) = \frac{1}{S}\iint_S \varepsilon(\boldsymbol{x})\, \mathrm{e}^{-\mathrm{i}\mathbf{G}\cdot\mathbf{x}} dS$$

$$\varepsilon_{eff} = \left(1-\frac{\pi r^2}{a^2}\right)\varepsilon_b + \pi r^2 \varepsilon_p$$

$$\omega = \sqrt{\frac{1}{\left(1-\frac{\pi r^2}{a^2}\right)\varepsilon_b + \frac{\pi r^2}{a}\varepsilon_p}}\sqrt{c^2\frac{\nabla\times\left(\nabla\times E(\boldsymbol{x},k)\right)}{E(\boldsymbol{x},k)}}$$

$$\omega = \sqrt{\frac{1}{\varepsilon_b - \frac{\pi r^2}{a}(\varepsilon_b-\varepsilon_p)}}\sqrt{c^2\frac{\nabla\times\left(\nabla\times E(\boldsymbol{x},k)\right)}{E(\boldsymbol{x},k)}}$$

$$\omega(r) \propto \sqrt{\frac{1}{A-Br^2}}$$

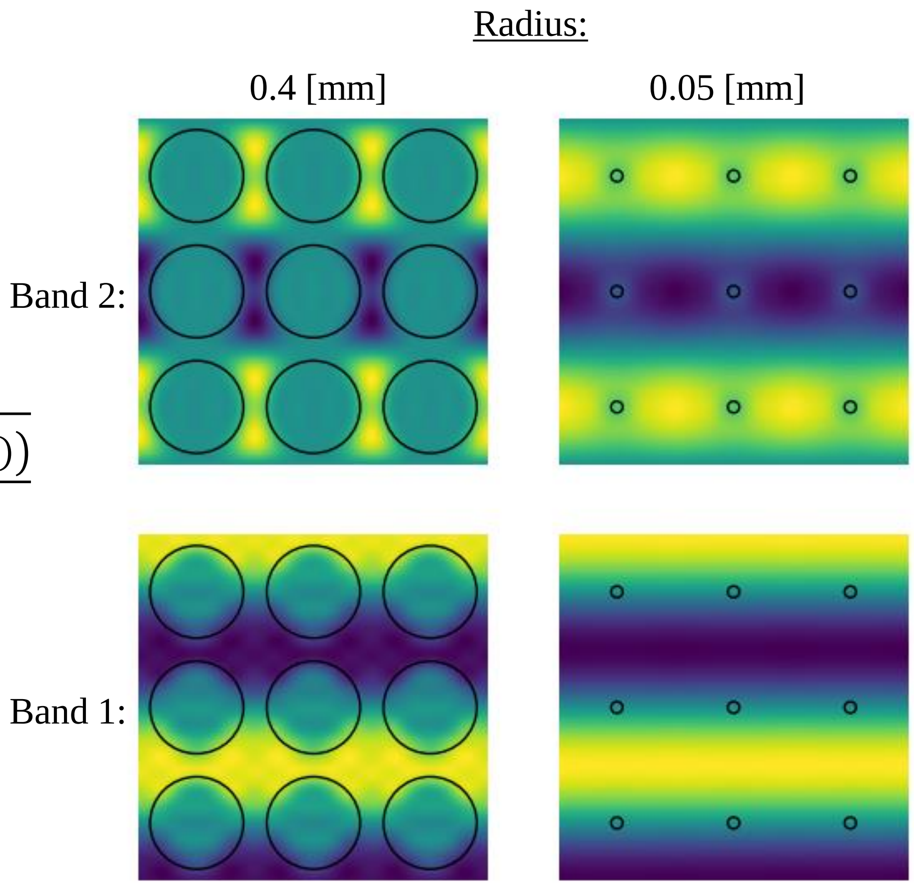

FIG 33. Electric field distributions of reference and final parameter value.

Wavevector along Γ-X, $k = \left\langle 0, \frac{\pi}{a} \right\rangle$

Lattice Constant

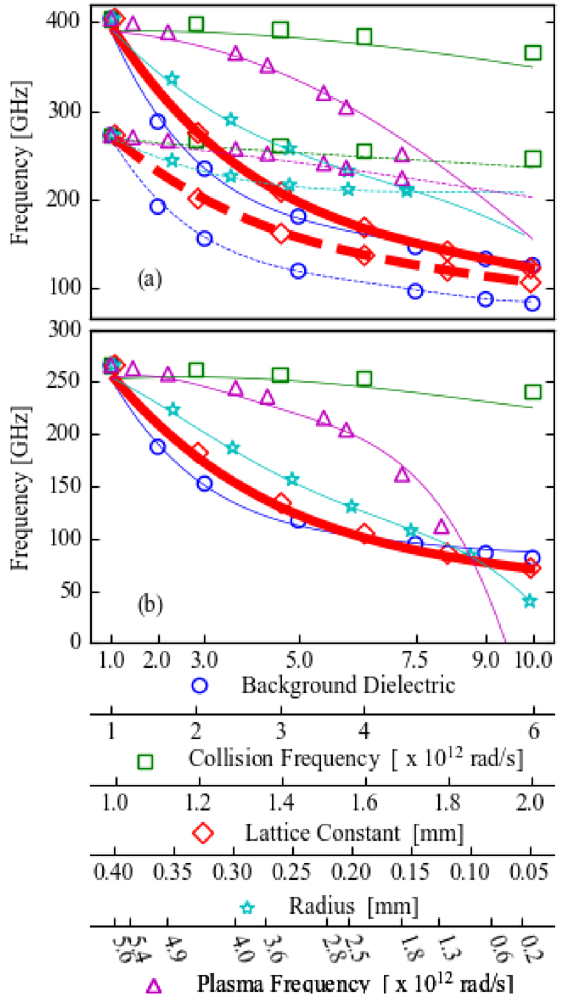

FIG 34. Parameter Trends: (a) Band Gap #2 and (b) Band Gap #1

$$\omega = \sqrt{c^2 \frac{\nabla \times \left(\nabla \times E(\boldsymbol{x}, k)\right)}{\varepsilon_{bg} E(\boldsymbol{x}, k)}}$$

$$\nabla \times \nabla \propto \frac{1}{a^2}$$

$$\omega(a) \propto \frac{1}{a}$$

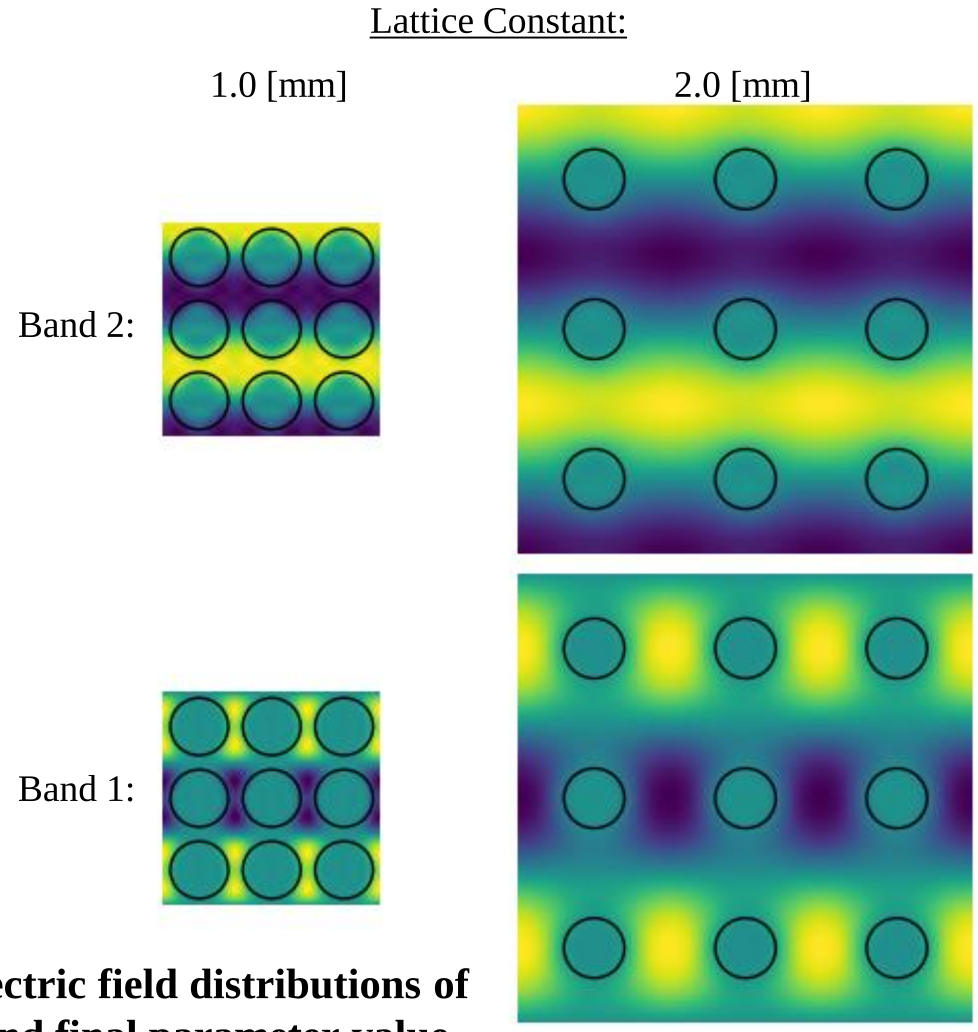

FIG 35. Electric field distributions of reference and final parameter value.

Wavevector along Γ-X, k = $\left\langle 0, \frac{\pi}{a} \right\rangle$

Reconfigurable Metrics

<u>Purpose:</u>

1) Measure "Reconfigurability"

2) Collectively visualize all data – 5D ranges:
   - Background Dielectric: 1.0 – 10.0
   - Collision Frequency: 0.2 – 5.0 [10^{12} rad/s]
   - Lattice Constant: 1.0 – 2.0 [mm]
   - Radius: 0.05 – 0.4 [mm]
   - Plasma Frequency: 0.2 – 5.0 [10^{12} rad/s]

3) Identify preferred parameters for:
   - Bandgap Width
   - Bandgap Center Frequency

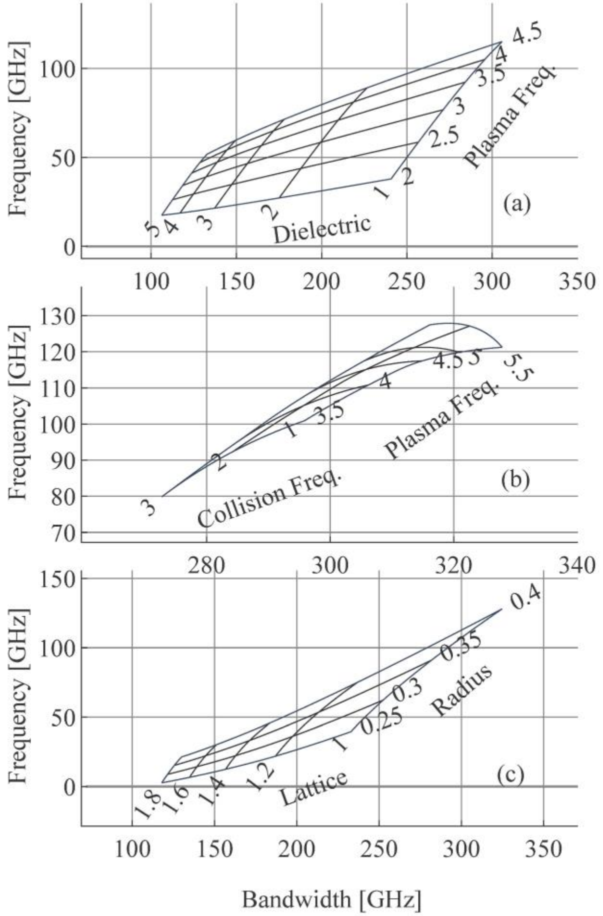

FIG 36. Bandgap center frequency and width per parameter values: Example of difficulty in displaying data graphically

Operational Range

Operational Range: The maximum and minimum frequencies when a single variable is held fixed and all other variables are allowed to vary over their respective ranges.

Minimums values for a bandgap

- Radius: 0.15 [mm]

- Plasma Frequency: 0.6 [10^{12} rad/s]

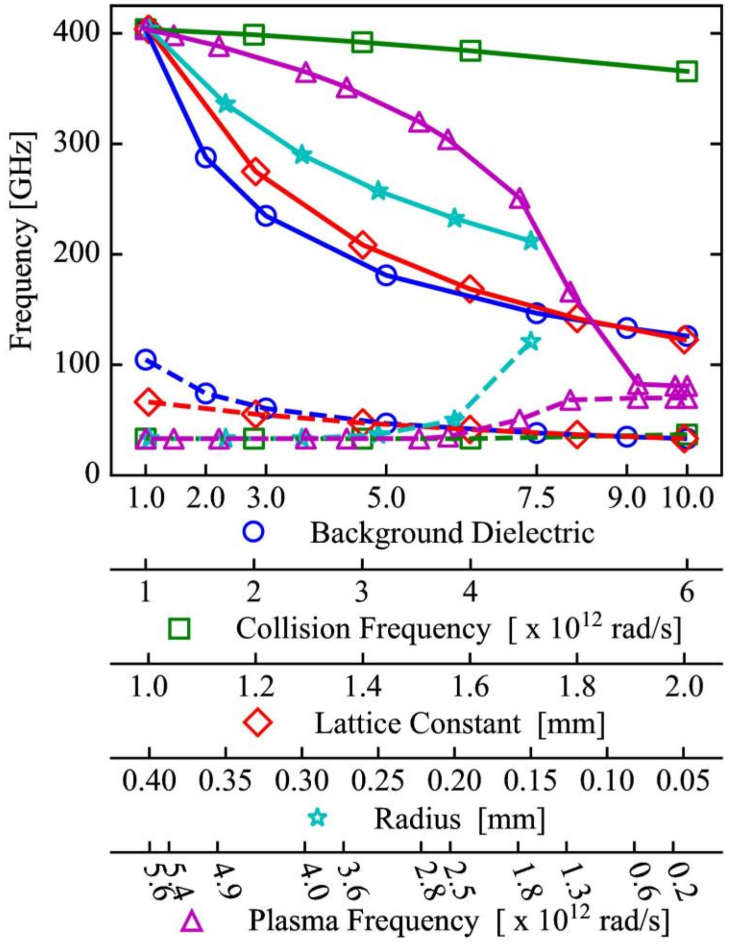

FIG 37. Operational range per parameter (Band Gap #2)

Parameter Sensitivity

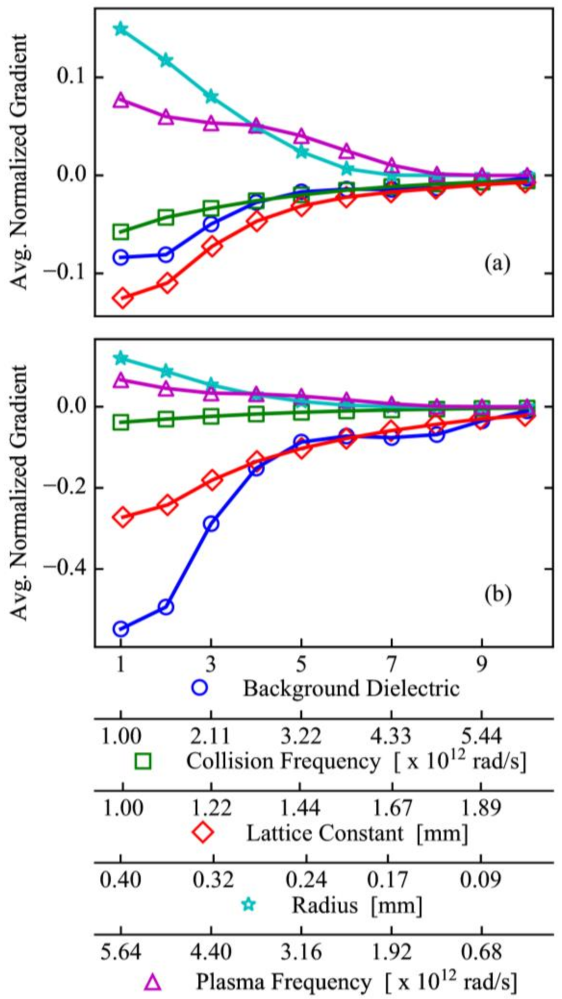

FIG 38. Parameter sensitivity over the range of the parameter (Band Gap #2): (a) Bandwidth and (b) Center Frequency

Table 1. Total parameter sensitivity parameter

Variables	Bandwidth	Center Frequency
Background Dielectric	-0.030	**-0.172**
Collision Frequency	-0.022	-0.015
Lattice Constant	**-0.043**	**-0.113**
Column Radius	**0.059**	0.041
Plasma Frequency	0.035	0.024

$$\langle \Delta x_1 \overline{\frac{1}{f}\frac{\partial f}{\partial x_1}}, \dots, \Delta x_n \overline{\frac{1}{f}\frac{\partial f}{\partial x_n}} \rangle = \frac{\int \dots \int \frac{\nabla f(x)}{f(x)}\, d^n x}{\int \dots \int\, d^n x} \cdot \langle \Delta x_1, \dots, \Delta x_n \rangle$$

Individual Intensity Controlled by Voltage Bias[25]

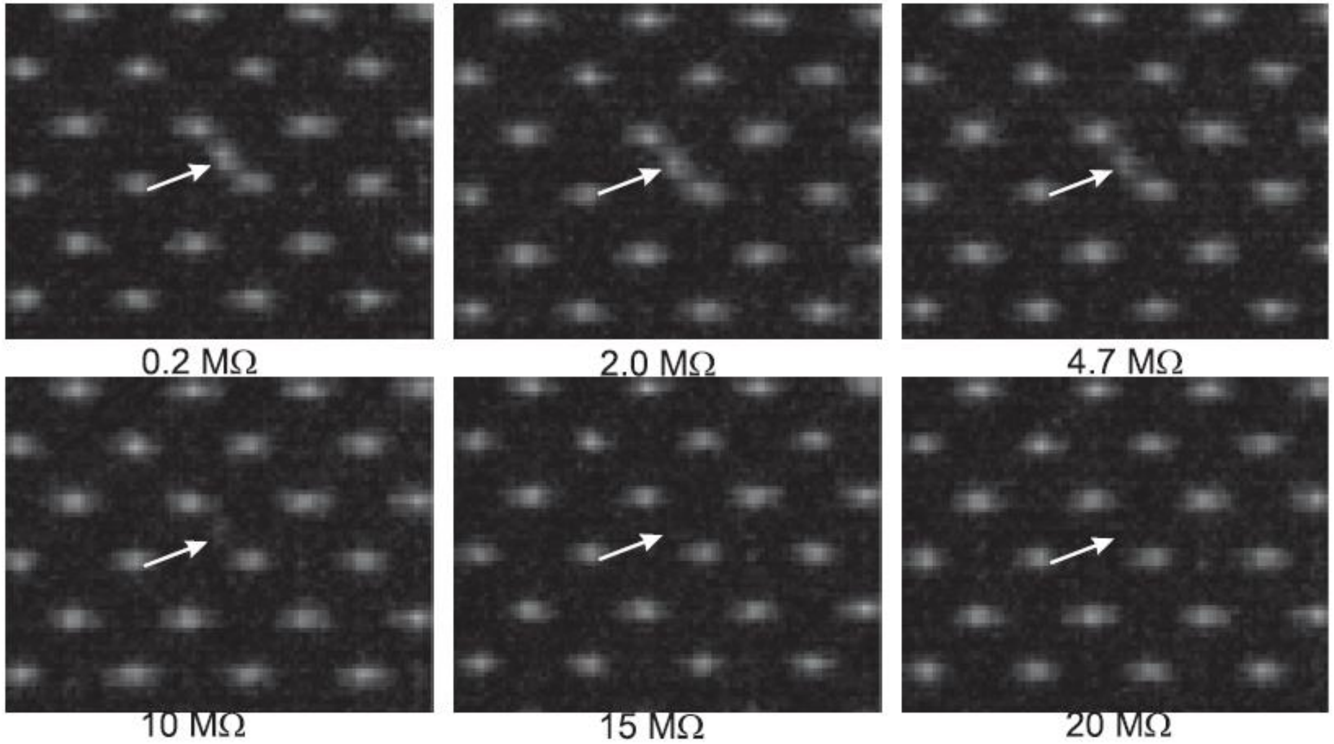

FIG 39. Decreasing light intensity with resistive voltage bias at pin

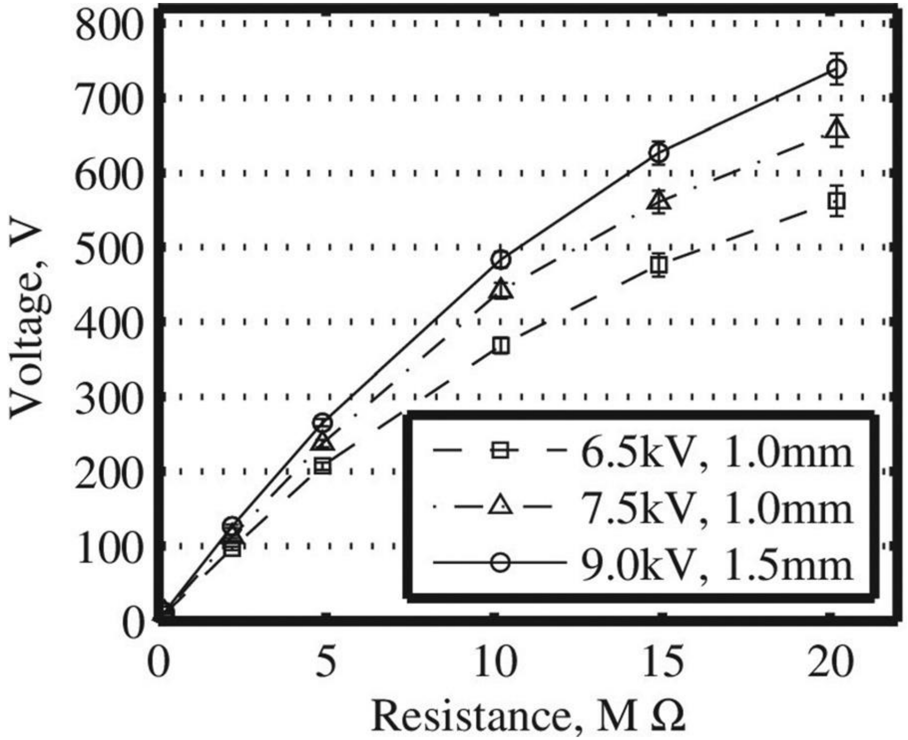

FIG 40. Bias voltage at pin per resistance. For different driving voltages and discharge gap widths.

Individually Addressable Filament Array
(Current Work)

FIG 41. Discharge:

- Volt: 6.5 kV
- Spacer: 1 mm
- Exp: 1/10 sec

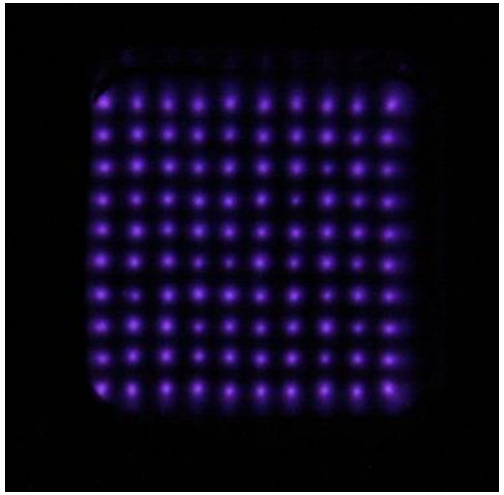

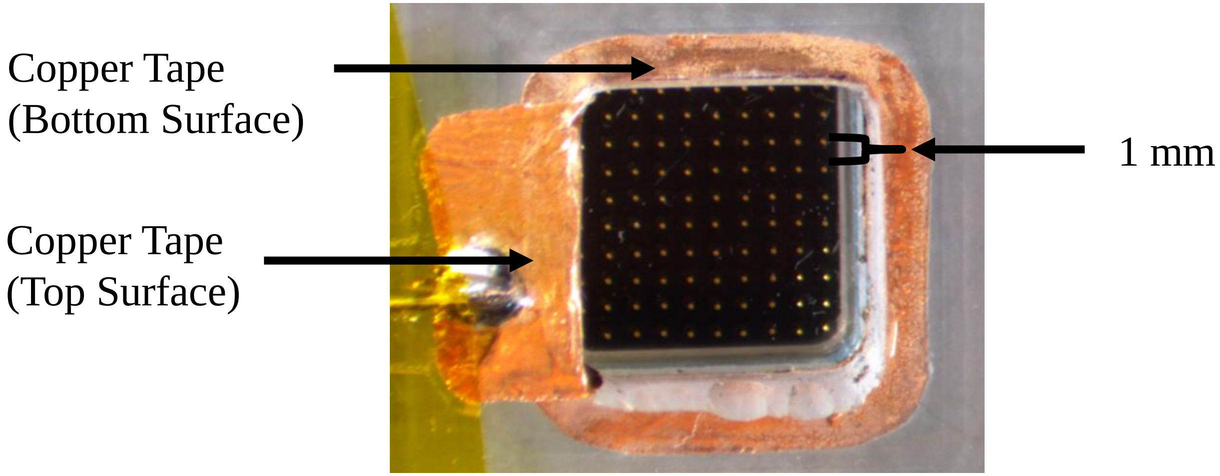

FIG 43. Top View

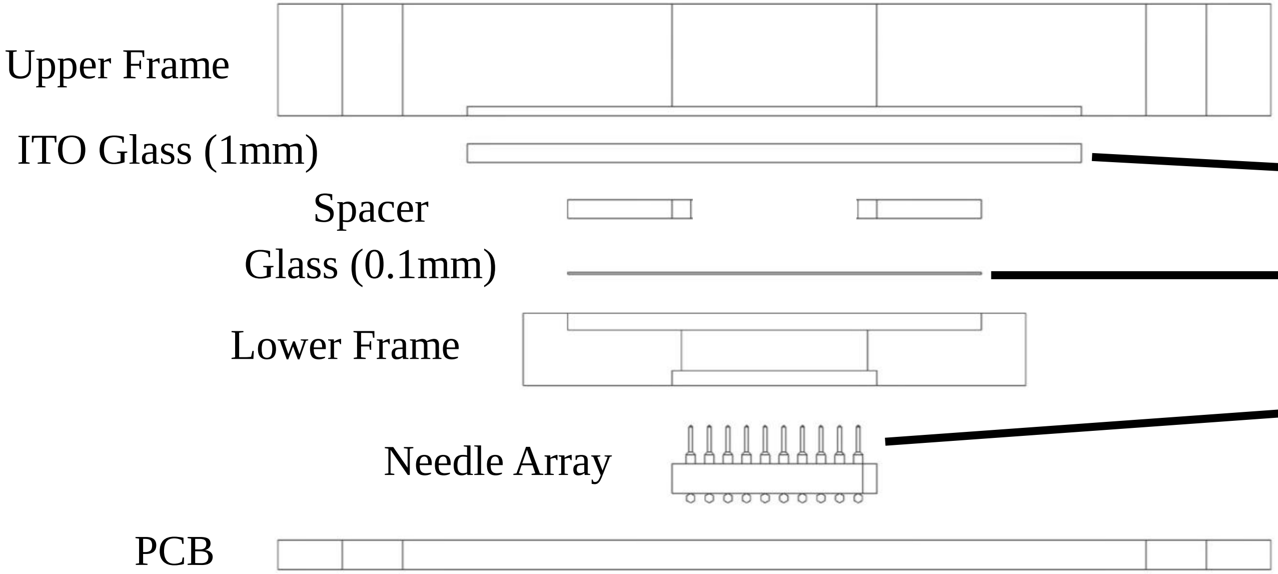

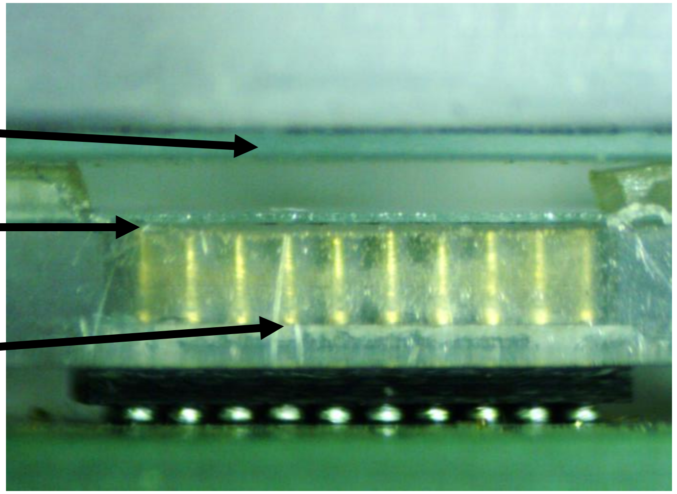

FIG 44. Side View

FIG 42. Exploded Schematic

Multiple Pin Control

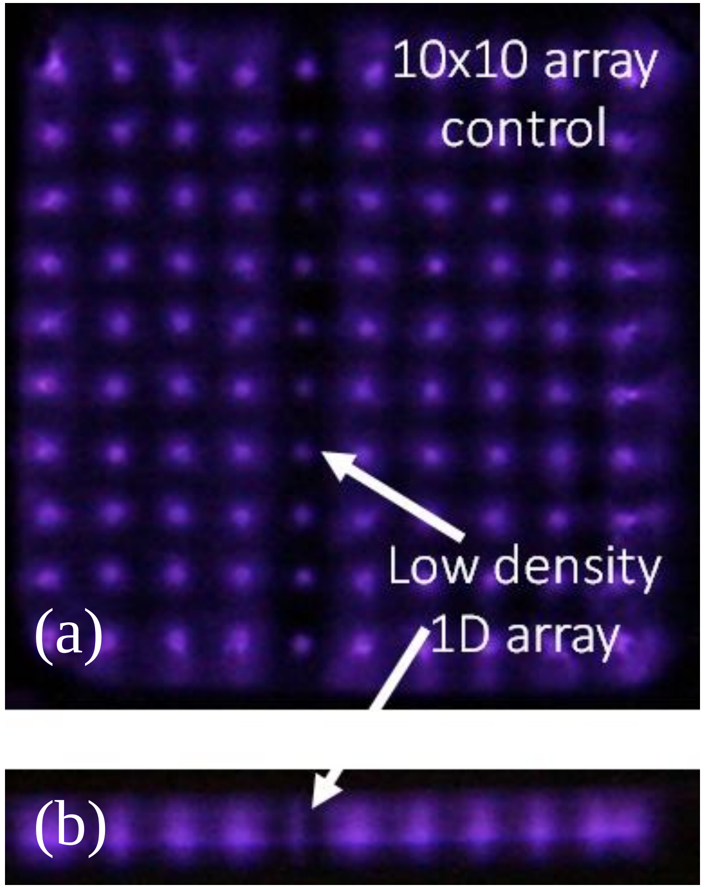

FIG 45. Multi-Pin Control PPC: (a) Top view through transparent electrode and (b) side view of filaments.

Current Work:

- Replace resistive bias with a transistor.
- Digitally control array.

Future Work:

- Experimental microwave validation

Goal of Individual Filament Control

FIG 46. Expand Parameter Control / Reconfigurability

Lattice Constant

Lattice Geometry

Background Dielectric

Radius

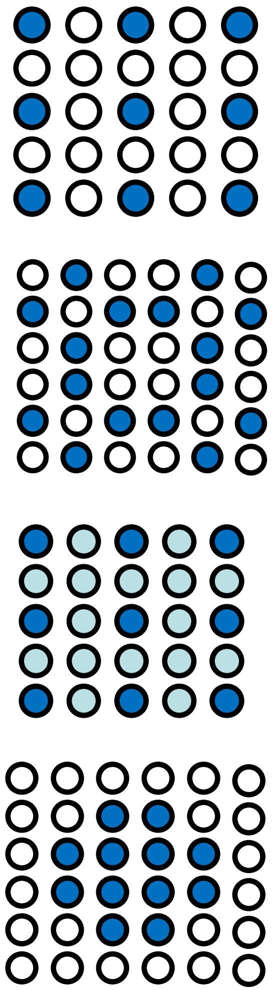

Summary

1. Review of Plasma Photonic Crystals
2. Bandgap - Parameter Trends
3. Preferred Bandgap Controlling Parameters:
   - Background Dielectric (Center Frequency)
   - Plasma Radius (Bandwidth)
4. Individual DBD Filament Control - Expand Reconfigurability

Partial funding provided by:

- Air Force Research Lab (Grant No. FA9451-17-1-0019) at Kirtland Air Force Base
- Department of Education GAANN Fellowship Program (award P200A180050-19)
- Directed Energy Graduate Scholarship 2019-2020

Bibliography

[1] L. Chien-Hao, J. D. Neher, J. H. Booske, and N. Behdad, IEEE Trans. Plasma Sci. 42, 1255 (2014)

[2] R. Seviour, Y. S. Tan, and A. Hopper, *8° International Congress on Advanced Electromagnetic Materials in Microwaves and Optics – Metamaterials 2014*, Copenhagen, Denamrk, 25-30 August 2014, Fig.3 A and B.

[3] J. Faith, S.P. Kuo, and J. Huang, Phys. Rev. E **55**, 1843 (1997)

[4] S.P. Kuo and J. Faith, Phys. Rev. E **56**, 2143 (1997)

[5] W. Fan and L. Dong, Phys. Plasmas 17, 073506 (2010)

[6] L. Zhang and J. T. Ouyang, Phys. Plasmas 21, 103514 (2014

[7] O. Sakai, T. Sakaguchi, and K. Tachibana, J. Appl. Phys. **101**, 073304 (2007)

[8] T. Sakaguchi, O. Sakai, and K. Tachibana, J. Appl. Phys. **101**, 073305 (2007)

[9] H. J. Yang *et al* 2017 *J. Phys. D: Appl. Phys.* **50** 43LT05

[10] B. Wang and M.A. Cappelli, AIP Adv. **6**, 065015 (2016)

[11] P. P. Sun, R. Zhang, W. Chen, P. V. Braun, and J. G. Eden, Appl. Phys. Rev. **6**, 041406 (2019)

[12] B. Wang, J. A. Rodriguez, and M. A. Cappelli, Plasma Sources Sci. Technol. **28** (2019) 02LT01

[13] E.H. Matlis, T.C. Corke, B. Neiswander, and A.J. Hoffman, J. Appl. Phys. **124**, 093104 (2018)

[14] W. Liu, L. Dong, Y. Wang, X. Zhang, and Y. Pan, Phys. Plasmas **21**, 113504 (2014)

[15] Y. Wang, L. Dong, W. Liu, Y. He, and Y. Li, Phys. Plasmas **21**, 073505 (2014)

[16] Y. Cui, L. Dong, X. Gao, L. Wei, W. Liu, J. Feng, and Y. Pan, Phys. Plasmas **24**, 083513 (2017)

[17] O. Sakai, J. Maeda, T. Shimomura, and K. Urabe, Phys. Plasmas **20**, 073506 (2013)

[18] H. F. Zhang, G. W. Ding, H. M. Li, and S. B. Liu, Phys. of Plasmas 22, 022105 (2015)

[19] H. F. Zhang , S. B. Liu, and X. K. Kong), J. Electromagnetic Waves and App., **27**, pg 1776, (2013)

[20] H. F. Zhang, S. B. Liu, and Y. C. Jiang, Physics of Plasmas 21, 092104 (2014)

Bibliography (cont.)

[21] Joannopoulos, S.G. Johnson, R.D. Meade, and J.N. Winn, *Photonic Crystals : Molding the Flow of Light* (Princeton University Press, Princeton, N.J., 1995)

[22] M. C. Paliwoda and J. L. Rovey, Phys. Plasmas, **27**, 023516 (2020)

[23] V. Kuzmiak and A. A. Maradudin, Phys. Rev. B. **55**, 7427 (1997)

[24] H. F. Zhang, G. W. Ding, H. M. Li, and S. B. Liu, Phys. Plasmas, **22**, 022105 (2015)

[25] M.C. Paliwoda and J.L. Rovey, Phys. Plasmas **24**, 053504 (2017).